

Concept-Aware LoRA for Domain-Aligned Segmentation Dataset Generation

Minho Park^{1,2*} Sunghyun Park¹ Jungsoo Lee¹ Hyojin Park¹
Kyuwoong Hwang¹ Fatih Porikli¹ Jaegul Choo² Sungha Choi^{1†}

¹Qualcomm AI Research[‡] ²KAIST

{m.park, jchoo}@kaist.ac.kr {sunpar, jungsool, hyojinp, kyuwoong, fporikli, sunghac}@qti.qualcomm.com

Abstract

This paper addresses the challenge of data scarcity in semantic segmentation by generating datasets through text-to-image (T2I) generation models, reducing image acquisition and labeling costs. Segmentation dataset generation faces two key challenges: 1) aligning generated samples with the target domain and 2) producing informative samples beyond the training data. Fine-tuning T2I models can help generate samples aligned with the target domain. However, it often overfits and memorizes training data, limiting their ability to generate diverse and well-aligned samples. To overcome these issues, we propose Concept-Aware LoRA (CA-LoRA), a novel fine-tuning approach that selectively identifies and updates only the weights associated with necessary concepts (e.g., style or viewpoint) for domain alignment while preserving the pretrained knowledge of the T2I model to produce informative samples. We demonstrate its effectiveness in generating datasets for urban-scene segmentation, outperforming baseline and state-of-the-art methods in in-domain (few-shot and fully-supervised) settings, as well as in domain generalization tasks, especially under challenging conditions such as adverse weather and varying illumination, further highlighting its superiority.

1. Introduction

The amount of labeled data is crucial for achieving high performance in semantic segmentation. However, acquiring diverse image samples, especially in rare or complex scenarios, and providing pixel-wise annotations are labor-intensive and time-consuming. Recent advances in text-to-image (T2I) generation models [37, 41, 43] have significantly improved image quality, enabling their use for data creation in perception tasks such as segmentation with minimal human effort. Recent studies [2, 51, 52, 59] leverage these models, such as Stable Diffusion [41], pretrained

on large-scale datasets [46]. By utilizing the rich generative features from T2I models, label generation modules can be trained with minimal labeled data to parse semantic regions. Furthermore, these models also provide controllability through text input, allowing for the generation of underrepresented distributions. These approaches have proven particularly effective in augmenting labeled datasets [1, 16, 51, 59], addressing data scarcity, and creating desired distributions, such as long-tailed class distributions [47] or adverse weather condition [23].

There are two primary challenges in generating segmentation datasets using image generation models: 1) aligning with the target domain, and 2) generating informative datasets beyond existing training data. However, previous approaches have overlooked key aspects of these issues. Existing methods [2, 29, 35, 59] typically produce domain-aligned but non-informative samples, as they train image generation models from scratch using only segmentation datasets, resulting in images that closely resemble the training data. To overcome this, leveraging T2I models such as Stable Diffusion, pretrained on large-scale datasets, is crucial for generating more diverse and informative samples. However, recent methods [23, 51, 52, 56] often use these pretrained models without fine-tuning for segmentation tasks, leading to poor alignment with the target domain.

Full fine-tuning or Low-Rank Adaptation (LoRA) [21] of pretrained T2I models are potential solutions to the challenges discussed above. However, as shown in Fig. 1, even LoRA fine-tuning often overfits and memorizes training data, limiting the generation of diverse and informative samples. This occurs because the model learns all concepts (e.g., viewpoint, style, object shape, and layout) existing in the training data. Therefore, we need a method to selectively learn only the necessary concepts (e.g., viewpoint or style) for domain alignment, while leveraging the pretrained knowledge of T2I models to generate informative samples.

The problem setting (e.g., in-domain or domain generalization (DG)) determines the target domain, affecting the concepts the model should learn during fine-tuning. In in-domain settings, the model needs to learn the style of the

*Work done during an internship at Qualcomm AI Research.

† Corresponding author. ‡ Qualcomm AI Research is an initiative of Qualcomm Technologies, Inc.

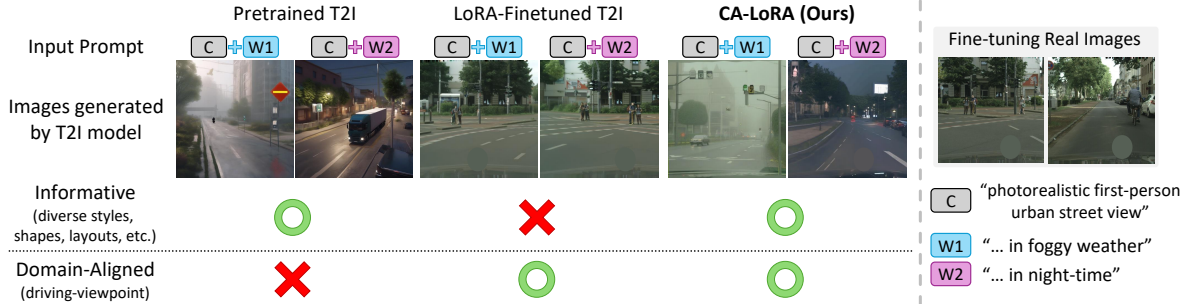


Figure 1. Motivation of Concept-Aware LoRA (CA-LoRA). Pretrained T2I models generate informative images but struggle with viewpoint alignment. LoRA fine-tuning on Cityscapes enables driving-viewpoint generation but leads to overfitting to the Cityscapes style and content. We aim to learn only the desired concept (*e.g.*, viewpoint) for generating domain-aligned, informative samples.

training data. However, in DG settings, where the target domain is unseen, learning only the viewpoint is more effective. For example, if the target domain is ACDC [45], which contains driving scenes under adverse weather conditions, learning all concepts from Cityscapes [9], containing only clear-day driving scenes, is suboptimal. Instead, the model should generate driving scenes (domain-aligned) under diverse weather conditions (informative) by learning only viewpoints from Cityscapes, excluding its clear-day style. However, as shown in Fig. 1, a pretrained model often fails to generate proper driving viewpoints, while a LoRA fine-tuned model generates only the clear-day style, even when ‘foggy’ or ‘night-time’ conditions are specified in the prompts. Therefore, a method that selectively learns only viewpoints from Cityscapes is necessary.

To the best of our knowledge, this is the first work to address these issues comprehensively. We propose Concept-Aware LoRA (CA-LoRA) that updates only the weights related to desired concepts (*e.g.*, viewpoint or style) while preserving the rest to leverage the knowledge of pretrained T2I models. Our approach enables the model to learn only the key concepts needed for aligning with the target domain, resulting in generated images that are not only well-aligned but also more diverse and informative. For example, if the desired concept is driving-scene viewpoints, the model learns that viewpoint alone and generates images that extend beyond the original training data by incorporating various styles, object shapes, and layouts. Additionally, the text controllability of T2I models enables the generation of specific styles from user input, making them highly effective in DG setting [7, 19, 20], which require diverse conditions such as adverse weather or varying illumination.

We demonstrate the effectiveness of our approach for urban-scene segmentation by comparing it with state-of-the-art dataset generation methods [4, 5, 23, 51] in both in-domain and DG settings. Our contributions are threefold:

1. We propose Concept-Aware LoRA, a novel fine-tuning method that selectively identifies and updates only the weights related to the necessary concepts (*e.g.*, viewpoint or style) for domain alignment, reducing overfit-

ting and preserving pretrained knowledge.

2. Concept-Aware LoRA enables T2I models to generate well-aligned and informative samples beyond training data. This addresses data scarcity by generating image-label pairs from underrepresented distributions (*e.g.*, adverse weather), improving segmentation performance.
3. Our method achieves state-of-the-art performance across various tasks, with improvements of +2.30 mIoU in few-shot, +1.34 mIoU in fully supervised settings on Cityscapes, and +1.53 mIoU in DG benchmarks (ACDC, Dark Zurich, BDD100K, Mapillary Vistas), along with strong results on Pascal-VOC. It consistently generates higher-quality image-label pairs than existing methods.

2. Related Work

2.1. Efficient Fine-Tuning of T2I Models

Recent advancements in diffusion architectures [18, 41] and large-scale image-text dataset [46] have enabled high-quality T2I models [11, 37, 39, 43]. The quality of images generated by these models has led researchers to personalize them to produce specific concepts or styles [13, 42]. To achieve better customization, parameter-efficient fine-tuning (PEFT) methods [10, 15, 17, 21, 27, 30] have been proposed. While existing PEFT methods aim to prevent overfitting and enable efficient training, they struggle to disentangle irrelevant concepts during fine-tuning, as they may still equally affect all layers. Thus, several studies [8, 14, 28] have shown that fine-tuning manually selected layers outperforms full fine-tuning, especially with smaller datasets. Additionally, recent work on Stable Diffusion [3, 50, 55] identifies control blocks for specific visual attributes by ablating each block manually. In contrast, our approach aims to automate this process, allowing precise, fine-grained updates to only the most crucial weights.

2.2. Segmentation Dataset Generation

Generating semantic segmentation datasets has been deeply explored, as pixel-wise annotations are particularly expensive. One classical approach to generating segmentation pairs is to create corresponding label maps for the images produced by image generation models [2, 29, 35, 59].

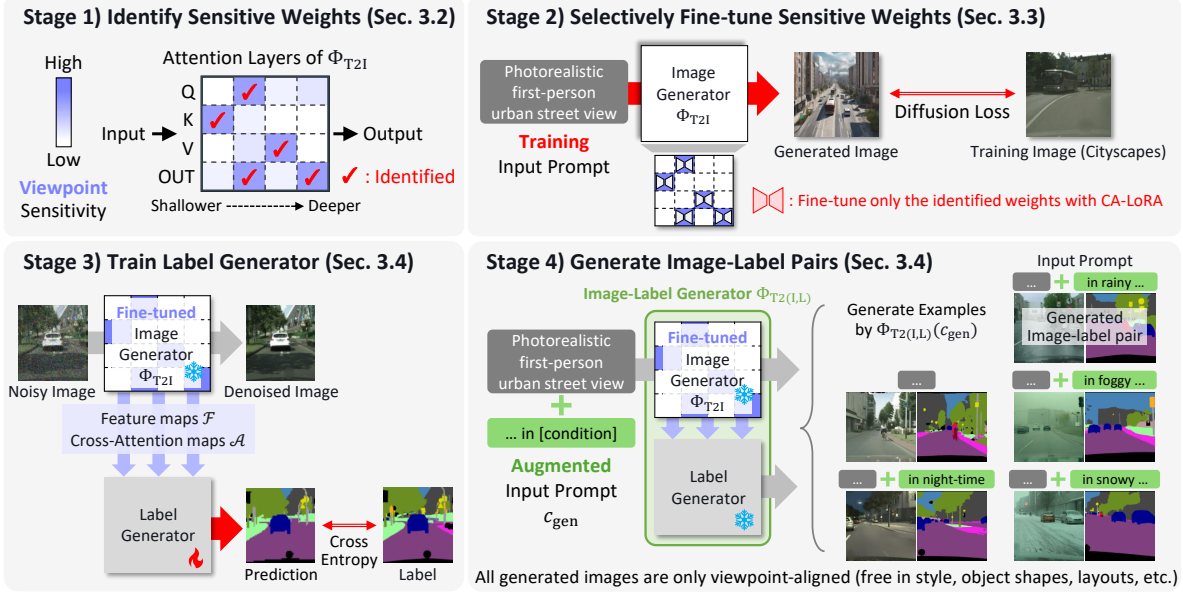


Figure 2. Overview of the proposed framework for generating an urban-scene segmentation dataset by learning the Cityscapes viewpoint. The process consists of four stages: (1) identifying sensitive weights for a specific concept, (2) selectively fine-tuning them with LoRA, (3) training a label generator using features from T2I model, and (4) generating diverse image-label pairs with augmented prompts.

Specifically, they utilized the intermediate features of the generative models (*e.g.*, GAN, DM) during image generation, which contains rich semantical information of the generated image. By leveraging these rich generative features, a label generator can be trained with minimal labeled data.

Recent studies have focused on leveraging the pretrained knowledge of T2I models [4, 34, 51, 52], but often overlook the alignment of the generated images with the target domain (*e.g.*, style, viewpoint). This paper explores the impact of fine-tuning T2I models for segmentation dataset generation, focusing on ensuring better image alignment.

3. Method

3.1. Overall Framework

Fig. 2 shows our dataset generation framework. First, we identify weights sensitive to the desired concept to be learned from the source dataset (Stage 1). Next, Concept-Aware LoRA selectively fine-tunes the top- $k\%$ sensitive weights of the T2I model (Stage 2). Then, a label generator is trained on a labeled dataset using rich image generative features from the T2I model (Stage 3). Finally, diverse image-label pairs are generated with augmented prompts according to the problem settings (Stage 4).

3.2. Identify Sensitive Weights to Desired Concept

To identify the sensitive weights for a specific concept (*e.g.*, style, viewpoint), we design an objective function, Concept loss ($\mathcal{L}_{\text{Concept}}$), which can be flexibly changed according to the desired concept. As shown in Fig. 3 (a), Concept loss is applied to the noisy image to enforce modifying the con-

cept. For example, when the Concept loss forces the T2I model to modify style (*e.g.*, photorealistic \rightarrow sketch), its gradient can be used to identify style-sensitive weights.

First, for the Concept loss input, we generate a few images x_0 using the T2I model Φ_{T2I} parameterized by θ and the text prompt c (*i.e.*, $x_0 = \Phi_{\text{T2I}}(c; \theta)$). Random Gaussian noise ϵ is then added to the images based on the pre-defined timestep t and the timestep scheduling coefficient $\bar{\alpha}_t$.¹

$$x_t = \sqrt{\bar{\alpha}_t}x_0 + \sqrt{1 - \bar{\alpha}_t}\epsilon, \quad \epsilon \sim \mathcal{N}(0, \mathbf{I}) \quad (1)$$

Then, we prepare the augmented versions of the original text prompt according to style and viewpoint. For example, when the original text prompt is given as

$$c = \text{“Photorealistic first-person urban street view”}, \quad (2)$$

we design **style-** and **viewpoint-**augmented prompts as follows:

$$c_{\text{Aug(Style)}} = \text{“Sketch of first-person urban street view”}, \quad (3)$$

$$c_{\text{Aug(Viewpoint)}} = \text{“Photorealistic urban street in top-down view”}. \quad (4)$$

We then use denoising prediction generated using the augmented caption as pseudo-ground truth to guide image modification. Concept loss ($\mathcal{L}_{\text{Concept}}$) is defined as follows, similar to the original diffusion loss.

$$\mathcal{L}_{\text{Concept}} := \|\epsilon_{\theta}(x_t, c, t) - \text{sg}[\epsilon_{\theta}(x_t, c_{\text{Aug}}, t)]\|_2^2, \quad (5)$$

where sg denotes the stop-gradient operation. Initially, we quantify concept sensitivity using the RMS norm of the concept loss gradient ($\|\nabla_{\theta} \mathcal{L}_{\text{Concept}}\|$) to compare gradients

¹The x_0 will be replaced to latent for the latent diffusion models [41].

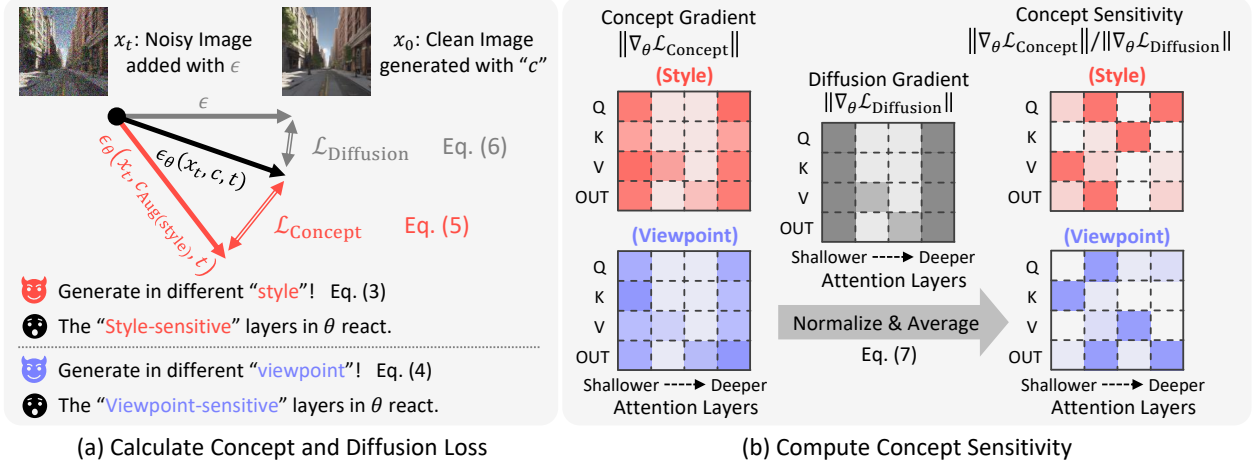


Figure 3. Overview of measuring concept sensitivity. (a) We design the concept loss ($\mathcal{L}_{\text{Concept}}$) with the concept-augmented captions (c_{Aug}), and the original diffusion loss ($\mathcal{L}_{\text{Diffusion}}$) with the added noise ϵ . The concept-augmented captions can be changed according to the desired concept (e.g., style, viewpoint). (b) While each concept gradient represents the reaction of the concept, it has to be normalized with the original diffusion gradient to assess the increased ratio of each layer.

across layers with different dimensions. However, gradients exhibit significant positional bias across layers (Supplementary Section B.1). To address this, we scale the gradient magnitude for each layer by computing the ratio between the gradients of the concept loss and the original diffusion loss ($\|\nabla_{\theta} \mathcal{L}_{\text{Diffusion}}\|$), referred to as *concept sensitivity*.

$$\mathcal{L}_{\text{Diffusion}} := \|\epsilon_{\theta}(x_t, c, t) - \epsilon\|_2^2 \quad (6)$$

$$\text{Concept Sensitivity}(\theta) := \mathbb{E}_{x_0, \epsilon, c_{\text{Aug}}} \left[\frac{\|\nabla_{\theta} \mathcal{L}_{\text{Concept}}\|}{\|\nabla_{\theta} \mathcal{L}_{\text{Diffusion}}\|} \right] \quad (7)$$

As shown in Eq. (7), we compute the average gradient ratio over generated images (x_0), added noise (ϵ), and augmented prompts (c_{Aug}). Concept sensitivity varies based on how partial derivatives with respect to each parameter are grouped, such as block-wise or layer-wise. We adopt a projection-wise approach (details in Supplementary Section G.2) to identify weights sensitive to the desired concept, enabling its selective learning by modifying the target of the diffusion loss.

3.3. Concept-Aware LoRA (CA-LoRA)

Based on the concept sensitivity, we introduce *Concept-Aware LoRA* (CA-LoRA), a novel parameter-efficient fine-tuning method that selectively updates only concept-aware weights while preserving other weights. CA-LoRA enables the model to learn the desired concept while retaining the pretrained knowledge of T2I models for other concepts.

We begin with Low-Rank Adaptation (LoRA) [21], a widely used fine-tuning method for large-scale pretrained T2I models. For a pretrained weight matrix $W_0 \in \mathbb{R}^{d \times k}$, LoRA constrains updates using low-rank decomposition, $W_0 + \Delta W = W_0 + BA$, where $B \in \mathbb{R}^{d \times r}$, $A \in \mathbb{R}^{r \times k}$ and the rank $r \ll \min(d, k)$. In the literature on fine-tuning T2I models, LoRA is commonly applied to all projection

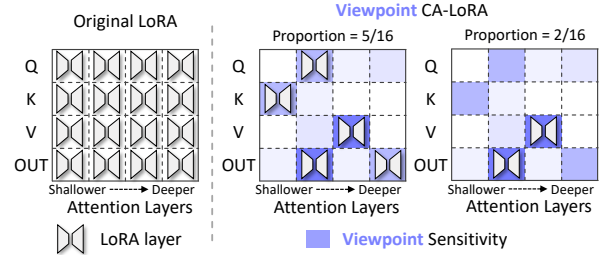


Figure 4. Illustration of CA-LoRA. Unlike the original LoRA, our CA-LoRA selectively attaches LoRA layers in a specified proportion to projection layers sensitive to the desired concept.

layers (Q, K, V, OUT) in each attention block of the pretrained T2I model [21, 41] (left in Fig. 4). LoRA and its extensions [40, 53, 58, 60] aim to improve parameter efficiency for better adaptation to downstream tasks (e.g., by refining low-rank matrix decomposition). However, selective learning approaches for a specific concept from given datasets have not been extensively explored.

CA-LoRA selectively fine-tunes the top- $k\%$ of pretrained weights based on concept sensitivity (Eq. (7)), enabling it to learn only the desired concept. Our experiments examine CA-LoRA in terms of viewpoint and style sensitivity. The selected proportions are user-adjustable, allowing control over the extent of fine-tuning, as shown in Fig. 4 (right). In the following sections, we refer to **Style CA-LoRA** and **Viewpoint CA-LoRA** as CA-LoRA fine-tuning based on style and viewpoint sensitivity, respectively.

3.4. Label Generator and Dataset Generation

Training Label Generator We train an additional lightweight label generator following DatasetDM [51] to produce a segmentation label corresponding to the image. First, given the real image x from the training set, we add noise to the real image x to synthesize noisy image

x_t . Then, we extract multi-scale generative features (feature maps \mathcal{F} , cross-attention maps \mathcal{A}) from the T2I generator $\epsilon_\theta(x_t, c, t)$, which contain lots of semantic information [24, 52, 59]. Last, the Mask2Former-shaped [6] label generator receives the generative features \mathcal{F} , \mathcal{A} and predicts the label maps as illustrated in Stage 3 of Fig. 2. In summary, the entire process can be encapsulated by the text-to-(image-and-label) generator, denoted as $\Phi_{T2(I,L)}$.

However, a significant domain gap exists between the training and generated images, as shown in Fig. 1. This difference results in generative features at inference exhibiting significantly different statistics from those at training, which in turn degrades the performance of the label generator. Unlike DatasetDM [51], we train the label generator using the fine-tuned T2I model with CA-LoRA. Since fine-tuning the T2I model on training images significantly reduces the domain gap, the label generator receives generative features at inference time that are statistically similar to those at training time, leading to a substantial improvement in image-label alignment.

Generating Diverse Dataset Lastly, we introduce a method to generate diverse image-label pairs by modifying text prompts. Generating adverse weather conditions (e.g., foggy, night-time) is crucial for improving domain generalization in urban-scene segmentation, as described in DGIn-Style [23]. To achieve this, we append weather conditions to the default prompt, e.g., “photorealistic first-person urban street view” to “... in foggy weather”, as illustrated in Stage 4 of Fig. 2. However, as shown in Fig. 1, fine-tuning T2I models with the original LoRA often leads to overfitting to undesired concepts from the source dataset (e.g., clear-day style from Cityscapes [9]) and compromises controllability over textual augmentation. In contrast, our CA-LoRA fine-tunes only the viewpoint-sensitive weights, enabling selective learning of viewpoint concepts while preserving the T2I model’s text adherence in style augmentation. This capability plays a critical role in generating diverse image-label pairs. Additionally, we vary class names in the prompt (e.g., “... with car, person, etc.”). In summary, the generation prompts are formulated as $c_{\text{Gen}} = \text{“Photorealistic first-person urban street view with [class names] in [weather condition].”}$. Now, the generated diverse dataset is utilized together with the real dataset to train segmentation models.

4. Experiments

This section presents extensive experiments on urban-scene segmentation in both in-domain and domain generalization (DG) settings. Section 4.1 describes the experimental setup and implementation details. Then, Section 4.2 presents extensive urban-scene segmentation experiments across in-

²Due to the absence of the source code with the generated datasets in Cityscapes as a source dataset, we cannot reproduce the reported results. However, we will update the table when the code is available.

domain and DG settings. Finally, Section 4.3 provides an in-depth analysis of the Concept-Aware LoRA (CA-LoRA), including a comprehensive ablation study.

4.1. Experimental Setup

Datasets For training, we use Cityscapes [9] as the source dataset for all urban-scene segmentation experiments, including in-domain and DG settings. Regarding the experiments for the in-domain few-shot setting, we only utilize a subset of Cityscapes images for the few-shot samples. For the evaluation, we test on Cityscapes (CS) validation set for in-domain, and ACDC [45], Dark Zurich (DZ) [44], BDD100K (BDD) [57], and Mapillary Vistas (MV) [33] for DG settings. Notably, ACDC and DZ are constructed with adverse weather conditions. We conduct additional experiments on Pascal-VOC [12] for general segmentation, with results provided in Supplementary Section D.

In-Domain Semantic Segmentation For baseline model, we train Mask2Former [6] on subsets of the Cityscapes [9] dataset at various fractions (0.3%, 1%, 3%, 10%, and 100%), which we denote as ‘Baseline’. Then, we generate 500 image-label pairs for all few-shot settings and use them as an additional dataset to fine-tune the baseline model, where we generate 3000 pairs for the fully-supervised setting. To prevent overfitting to the generated data, we mix real (e.g., samples from the Cityscapes dataset) and generated samples in equal proportions within each mini-batch. We compare our proposed approach with the segmentation dataset generation approach, DatasetDM [51], which utilizes the pretrained T2I model [41] without any fine-tuning. We include an additional baseline denoted as ‘Baseline (FT)’ that fine-tunes the baseline model exclusively on the same real dataset, ensuring a fair comparison in terms of the number of training iterations.

Domain Generalization in Semantic Segmentation We improve the DG performance for urban-scene segmentation by building upon existing DG methods, including ColorAug, DAFormer [19] and HRDA [20]. To show the effectiveness of the generated dataset, we train a semantic segmentation model with each DG method on a combination of the 2975 Cityscapes image-label pairs and the 2500 generated image-label pairs (500 images for 5 weather conditions including clear, foggy, night-time, rainy, and snowy) from scratch. We compare our approach with various dataset generation approaches, including DatasetDM [51], DGIn-Style [23], DATUM [4], and InstructPix2Pix [5].³

Implementation Details Throughout our experiments, we use Stable Diffusion XL [37] as the pretrained T2I model. For a fair comparison, we reimplement DatasetDM [51]

³For DATUM [4], we provide an additional image for each weather condition to meet the requirements of the one-shot UDA setting. For InstructPix2Pix [5], we modify the weather conditions of the images using instruction prompts (e.g., “change the weather condition to {...}”) while preserving the original segmentation maps.

Method	Training Dataset		Total Iterations	Fraction of the Cityscapes Dataset				
	Real	Generated		0.3%	1%	3%	10%	100%
Baseline	✓	✗	90K	41.83	49.15	59.07	69.02	79.40
For a fair comparison, we fine-tune the baseline for additional 30K iterations using real or generated datasets.								
Baseline (FT)	✓	✗	120K	42.00 (+0.17)	49.18 (+0.03)	59.06 (-0.01)	68.68 (-0.34)	80.05 (+0.65)
DatasetDM	✓	✓	120K	42.82 (+0.99)	49.71 (+0.56)	60.31 (+1.24)	69.04 (+0.02)	80.45 (+1.05)
Ours	✓	✓	120K	44.13 (+2.30)	51.90 (+2.75)	61.29 (+2.22)	70.29 (+1.27)	80.74 (+1.34)

Table 1. In-domain segmentation performance across various fractions of the Cityscapes dataset (mIoU). In the first row, we trained Mask2Former on various fractions of the Cityscapes dataset (Baseline). Then, we fine-tuned the baseline on DatasetDM and our generated datasets with 30K iterations and evaluated the performance of the fine-tuned segmentation models. Additionally, we include an additional fine-tuned baseline denoted as Baseline (FT), solely fine-tuned on the same real dataset for a fair comparison in terms of the total iterations.

DG Method	Generated Dataset	ACDC	DZ	BDD	MV	Average
ColorAug*	✗	52.38	23.00	53.33	60.06	47.19
ColorAug*	DGInStyle	55.19	26.83	55.18	59.95	49.29 (+2.10)
ColorAug	✗	53.12	25.69	53.00	59.81	47.91
ColorAug	DatasetDM	53.80	27.70	53.54	60.75	48.95 (+1.04)
ColorAug	InstructPix2Pix	56.02	26.92	54.03	60.44	49.35 (+1.44)
ColorAug	Ours	56.07	29.75	54.35	61.40	50.39 (+2.49)
DAFormer*	✗	55.15	28.28	54.19	61.67	49.82
DAFormer*	DGInStyle	57.74	28.55	56.26	62.67	51.31 (+1.48)
DAFormer	✗	53.98	27.82	54.29	62.69	49.70
DAFormer	DatasetDM	55.24	28.44	54.40	63.18	50.32 (+0.62)
DAFormer	InstructPix2Pix	55.13	26.93	54.61	62.36	49.76 (+0.06)
DAFormer	DATUM†	54.06	27.10	54.74	62.40	49.58 (-0.12)
DAFormer	Ours	55.83	31.68	54.68	63.09	51.32 (+1.63)
HRDA*	✗	59.70	31.07	58.49	68.32	54.40
HRDA*	DGInStyle	61.00	32.60	58.84	67.99	55.11 (+0.71)
HRDA	✗	58.48	29.46	56.12	64.27	52.08
HRDA	DatasetDM	58.11	31.51	55.74	64.49	52.46 (+0.38)
HRDA	InstructPix2Pix	58.50	29.56	56.10	64.10	52.07 (-0.01)
HRDA	DATUM†	58.11	30.18	56.94	64.29	52.38 (+0.30)
HRDA	Ours	58.93	34.41	56.56	64.54	53.61 (+1.53)

Table 2. Comparison of generated datasets for domain generalization (DG) in urban-scene segmentation (Cityscapes [9] → ACDC [45], Dark Zurich [44], BDD100K [57], Mapillary Vistas [33]) (mIoU). The experiments are conducted upon various DG methods (ColorAug [54], DAFormer [19], and HRDA [20]). * The gray color indicates the reported score from the DGInStyle authors.²†DATUM additionally leverages a single target domain image for each weather condition from the ACDC dataset.

with SDXL as well. We fix the rank of both the original LoRA and CA-LoRA at 64 and set the training iterations to 10k. While our method requires additional fine-tuning of the T2I model, increasing training time compared to DatasetDM, this process (*i.e.*, CA-LoRA fine-tuning) takes only one hour on a single Tesla V100 GPU, incurring minimal computational cost. Thus, its overhead remains marginal compared to the 20-hour training time of the label generator. We explore the selected proportion of CA-LoRA across 1%, 2%, 3%, 5%, and 10%, since 0% and 100% represent DatasetDM and the original LoRA, respectively. The diffusion timestep t for identifying the desired concept is set to 81 out of 1000 timesteps. The results of our hyper-parameter search, along with details such as the label generator architecture, are provided in Section G.

4.2. Main Results on the Segmentation Benchmarks

This section demonstrates the superiority of CA-LoRA in improving urban-scene segmentation performance through

both quantitative and qualitative results.

In-Domain Semantic Segmentation Table 1 shows that the proposed CA-LoRA consistently outperforms all other methods across various data ratios. Specifically, the proposed method improves mIoU by 2.30 for the 0.3% fraction of the Cityscapes, significantly surpassing DatasetDM, which achieves only a 0.99 mIoU increase. This demonstrates the efficiency of CA-LoRA, particularly in low-data regimes. Furthermore, our method improves the fully-supervised performance (*i.e.*, 100% data ratio) by 1.34 mIoU, further enhancing strong Mask2Former performance. The consistent gains across different data ratios highlight the robustness of CA-LoRA, making it highly effective for urban-scene segmentation in both few-shot and fully supervised settings.

Domain Generalization in Semantic Segmentation As shown in Table 2, the proposed method consistently outperforms all other segmentation dataset generation methods across multiple DG methods. Specifically, Viewpoint CA-

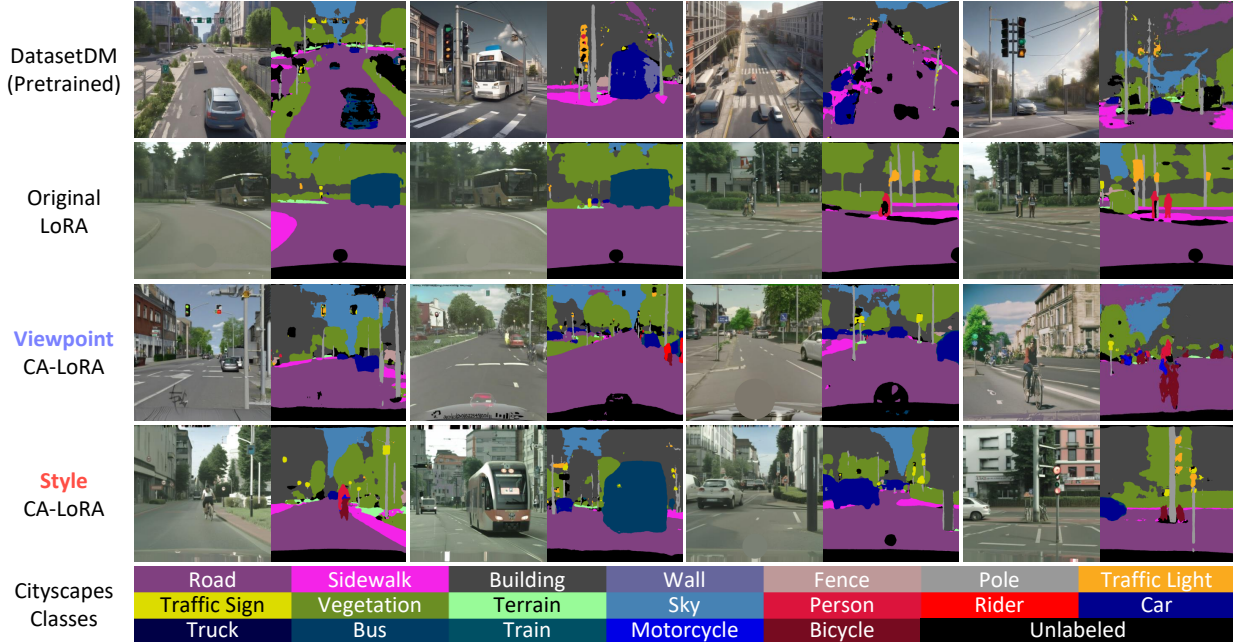


Figure 5. Qualitative comparison of image-label pairs between DatasetDM, Original LoRA, and our CA-LoRAs in a few-shot setting (Cityscapes, 0.3%). The pretrained model misaligns with the viewpoint and style of the target domain, while the original LoRA memorizes training examples. In contrast, CA-LoRA selectively learns either style or viewpoint concepts from the source dataset.

LoRA effectively learns only the viewpoint from the source dataset (Cityscapes) while maintaining the ability to generate diverse styles from the pretrained T2I model. As a result, our method significantly improves generalization performance, particularly on challenging datasets such as ACDC and Dark Zurich, where conditions such as adverse weather play a critical role. We emphasize that DGInStyle and InstructPix2Pix only change the styles of given images while keeping fixed label maps, which introduces limited manipulation of the scene. Since DAFormer and HRDA already employ strong image augmentation techniques [19, 20], the additional simplistic image augmentations from DGInStyle and InstructPix2Pix are largely redundant, as shown in their performance. In contrast, the improvement of the proposed approach is notable not only in comparison to the simple baseline (ColorAug) but also in its effectiveness on the advanced DG methods (DAFormer and HRDA) since our generated datasets contain semantically diverse content.

4.3. Analysis

This section presents an in-depth analysis of CA-LoRA finetuned models (style and viewpoint), comparing them to the pretrained base model and the original LoRA finetuned model. We first analyze the effective style adaptation of the Style CA-LoRA, then examine whether Viewpoint CA-LoRA maintains conditional image generation ability. Finally, we show a comprehensive ablation study for in-domain and DG for urban-scene segmentation across the pretrained model, CA-LoRA finetuned models (style, viewpoint), and the original LoRA finetuned model. Further

analyses of concept sensitivity and CA-LoRA are provided in Supplementary Sections B and C, respectively. Class-specific generation, including focusing on a specific class and exploring diverse class names, is presented in Supplementary Section F.

Image Domain Alignment We evaluate the image domain alignment of T2I models, which is crucial for generating an in-domain dataset. To assess the image domain alignment, we adopt CMMD [22] due to the reliability of maximum mean discrepancy in comparing small image sets. Table 3 shows that the pretrained T2I model exhibits a significant domain gap between real and generated images, whereas fine-tuning on Cityscapes effectively reduces this gap. Among CA-LoRAs, Style CA-LoRA achieves competitive image domain alignment with only 10% of the finetuned parameters of the original LoRA. While the original LoRA performs best in the CMMD metric, Fig. 1 highlights its memorization issue, which we further analyze in the following ablation study to demonstrate the limitations of the memorized dataset.

Image Generation for Various Weather Scenarios Since generating diverse weather conditions (*e.g.*, foggy, rainy) is crucial for improving DG performance, preserving the text adherence ability of the T2I model is essential. We measure the weather-conditional image generation performance by leveraging CLIP-Score [38], which can assess the similarity between the generated images and their input text prompts. Table 3 shows the average CLIP-Score across four diverse weather conditions, based on 100 gen-

Metric	Desired Concept	Proportion of T2I Model Layers for Concept-Aware Fine-tuning						
		0% (Pretrained)	1%	2%	3%	5%	10%	100% (Original LoRA)
CMMD	Style	5.063	1.618	1.420	1.021	1.105	0.686	0.644
	Viewpoint		2.650	2.313	1.580	1.733	1.476	
CLIP Score	Style	25.72	21.44	19.92	20.74	19.72	19.86	22.66
	Viewpoint		25.03	24.69	25.88	25.52	24.76	
Image-Label Alignment (mIoU)	Style	25.18	37.01	39.37	40.94	47.84	48.86	60.10
	Viewpoint		33.27	29.42	31.44	34.94	38.28	

Table 3. Evaluating generated datasets according to the desired concepts and the proportion of T2I model layers for concept-aware finetuning in a few-shot setting (Cityscapes, 0.3%). The generated datasets are measured by image domain alignment (CMMD ↓), fidelity of the weather-augmented prompts (CLIP-Score ↑), and image-label alignment (mIoU ↑).

Additional Generated Dataset	In-domain (0.3%)	Domain Generalization (ColorAug)				
	Cityscapes	ACDC	DZ	BDD	MV	Average
-	41.83	53.12	25.69	53.00	59.81	47.91
Pretrained (DatasetDM)	42.82 (+0.99)	53.80	27.70	53.54	60.75	48.95 (+1.04)
Original LoRA	42.97 (+1.14)	54.25	28.42	54.34	61.42	49.61 (+1.70)
Style CA-LoRA	44.13 (+2.30)	52.55	26.42	54.04	61.81	48.71 (+0.80)
Viewpoint CA-LoRA	43.13 (+1.30)	56.07	29.75	54.35	61.40	50.39 (+2.48)

Table 4. Ablation study of CA-LoRA on the in-domain (Cityscapes, 0.3%) and domain generalization (ColorAug, CS → ACDC, DZ, BDD, MV) settings (mIoU). Style CA-LoRA demonstrates significant improvements in the in-domain setting and Viewpoint CA-LoRA outperforms in the domain generalization setting.

erated images per condition. The results indicate that the pretrained model achieves a high CLIP score for generating adverse weather conditions, whereas the original LoRA and Style CA-LoRA fail to do so, as they primarily learn styles from the source dataset, which inherently includes its weather condition (*e.g.*, clear-day weather). In contrast, the Viewpoint CA-LoRA effectively preserves the adverse weather conditional generation performance while learning the viewpoint from the source dataset.

Image-Label Alignment To further demonstrate the effectiveness of our method, we analyze image-label alignment. As shown in Fig. 5 and Table 3, our method outperforms baselines both qualitatively and quantitatively by fine-tuning the T2I model with CA-LoRA for domain alignment. This ensures that generative features at inference are similar to those used during label generator training. To quantitatively measure performance with mIoU, we use the predicted label of Mask2Former [6] from the generated image of the T2I model as pseudo ground truth. Details are provided in Supplementary Section E.

Ablation Study We conduct an ablation study on CA-LoRA for both in-domain (Cityscapes, 0.3%) and DG (CS → ACDC, DZ, BDD, MV) settings. As shown in Table 4, the pretrained model and original LoRA show poor performance due to domain misalignment and memorization, respectively. In contrast, our Style CA-LoRA achieves a significant performance improvement of 2.30 by learning in-domain styles while preserving pretrained knowledge, enabling the generation of diverse scenes. Furthermore, as shown in Table 4, the Viewpoint CA-LoRA shows a sig-

nificant improvement of 2.48 on average for domain generalization. While the original LoRA and Style CA-LoRA show competitive performance improvements on BDD and MV, Viewpoint CA-LoRA significantly outperforms ACDC and DZ, which contain images under challenging weather conditions. These results show the strength of Viewpoint CA-LoRA in synthesizing adverse weather conditions.

5. Conclusion and Future Work

This paper proposes Concept-Aware LoRA (CA-LoRA), a novel fine-tuning method that learns only the desired concepts (*e.g.*, viewpoint or style) from the training dataset to generate segmentation datasets. By selectively identifying and updating only the weights relevant to the desired concepts, CA-LoRA enables the fine-tuned T2I model to produce well-aligned and informative samples. Moreover, it effectively leverages pretrained knowledge from T2I models to generate datasets, significantly improving segmentation performance across various settings, including in-domain (few-shot and fully-supervised) and domain generalization tasks. While our experiments primarily focus on urban-scene segmentation, additional experiments on PASCAL-VOC [12] demonstrate the general applicability of CA-LoRA (Supplementary Section D). Furthermore, CA-LoRA excels at learning only the desired concepts from training data, even when it contains diverse information, including unnecessary concepts for dataset generation, making it applicable to various knowledge transfer and fine-tuning tasks. As a promising future direction, our approach could be extended to extract specific concepts beyond style and viewpoint, enabling more personalized image generation.

References

- [1] Shekoofeh Azizi, Simon Kornblith, Chitwan Saharia, Mohammad Norouzi, and David J Fleet. Synthetic data from diffusion models improves imagenet classification. *arXiv preprint arXiv:2304.08466*, 2023. 1
- [2] Dmitry Baranchuk, Andrey Voynov, Ivan Rubachev, Valentin Khruikov, and Artem Babenko. Label-efficient semantic segmentation with diffusion models. In *International Conference on Learning Representations*, 2022. 1, 2
- [3] Samyadeep Basu, Keivan Rezaei, Priyatham Kattakinda, Vlad I Morariu, Nanxuan Zhao, Ryan A Rossi, Varun Manjunatha, and Soheil Feizi. On mechanistic knowledge localization in text-to-image generative models. In *Forty-first International Conference on Machine Learning*, 2024. 2
- [4] Yasser Benigmim, Subhankar Roy, Slim Essid, Vicky Kalogeiton, and Stéphane Lathuilière. One-shot unsupervised domain adaptation with personalized diffusion models. In *Proceedings of the IEEE/CVF conference on computer vision and pattern recognition*, pages 698–708, 2023. 2, 3, 5, 7
- [5] Tim Brooks, Aleksander Holynski, and Alexei A Efros. Instructpix2pix: Learning to follow image editing instructions. In *Proceedings of the IEEE/CVF Conference on Computer Vision and Pattern Recognition*, pages 18392–18402, 2023. 2, 5
- [6] Bowen Cheng, Ishan Misra, Alexander G Schwing, Alexander Kirillov, and Rohit Girdhar. Masked-attention mask transformer for universal image segmentation. In *Proceedings of the IEEE/CVF conference on computer vision and pattern recognition*, pages 1290–1299, 2022. 5, 8, 10, 16
- [7] Sungha Choi, Sanghun Jung, Huiwon Yun, Joanne T Kim, Seungryong Kim, and Jaegul Choo. Robustnet: Improving domain generalization in urban-scene segmentation via instance selective whitening. In *Proceedings of the IEEE/CVF conference on computer vision and pattern recognition*, pages 11580–11590, 2021. 2
- [8] Sungha Choi, Seunghan Yang, Seokeon Choi, and Sungrack Yun. Improving test-time adaptation via shift-agnostic weight regularization and nearest source prototypes. In *European Conference on Computer Vision*, pages 440–458. Springer, 2022. 2
- [9] Marius Cordts, Mohamed Omran, Sebastian Ramos, Timo Rehfeld, Markus Enzweiler, Rodrigo Benenson, Uwe Franke, Stefan Roth, and Bernt Schiele. The cityscapes dataset for semantic urban scene understanding. In *Proc. of the IEEE Conference on Computer Vision and Pattern Recognition (CVPR)*, 2016. 2, 5, 6, 4, 8
- [10] Ning Ding, Xingtai Lv, Qiaosen Wang, Yulin Chen, Bowen Zhou, Zhiyuan Liu, and Maosong Sun. Sparse low-rank adaptation of pre-trained language models. *arXiv preprint arXiv:2311.11696*, 2023. 2
- [11] Patrick Esser, Sumith Kulal, Andreas Blattmann, Rahim Entezari, Jonas Müller, Harry Saini, Yam Levi, Dominik Lorenz, Axel Sauer, Frederic Boesel, et al. Scaling rectified flow transformers for high-resolution image synthesis. In *Forty-first International Conference on Machine Learning*, 2024. 2
- [12] Mark Everingham, Luc Van Gool, Christopher KI Williams, John Winn, and Andrew Zisserman. The pascal visual object classes (voc) challenge. *International journal of computer vision*, 88:303–338, 2010. 5, 8, 1
- [13] Rinon Gal, Yuval Alaluf, Yuval Atzmon, Or Patashnik, Amit H Bermano, Gal Chechik, and Daniel Cohen-Or. An image is worth one word: Personalizing text-to-image generation using textual inversion. *arXiv preprint arXiv:2208.01618*, 2022. 2
- [14] Yunhui Guo, Honghui Shi, Abhishek Kumar, Kristen Grauman, Tajana Rosing, and Rogerio Feris. Spottune: transfer learning through adaptive fine-tuning. In *CVPR*, 2019. 2
- [15] Soufiane Hayou, Nikhil Ghosh, and Bin Yu. Lora+: Efficient low rank adaptation of large models. *arXiv preprint arXiv:2402.12354*, 2024. 2
- [16] Ruifei He, Shuyang Sun, Xin Yu, Chuhui Xue, Wenqing Zhang, Philip Torr, Song Bai, and XIAOJUAN QI. Is synthetic data from generative models ready for image recognition? In *The Eleventh International Conference on Learning Representations*, 2022. 1
- [17] Shwai He, Liang Ding, Daize Dong, Miao Zhang, and Dacheng Tao. Sparseadapter: An easy approach for improving the parameter-efficiency of adapters. *arXiv preprint arXiv:2210.04284*, 2022. 2
- [18] Jonathan Ho, Ajay Jain, and Pieter Abbeel. Denoising diffusion probabilistic models. *Advances in neural information processing systems*, 33:6840–6851, 2020. 2
- [19] Lukas Hoyer, Dengxin Dai, and Luc Van Gool. Daformer: Improving network architectures and training strategies for domain-adaptive semantic segmentation. In *Proceedings of the IEEE/CVF conference on computer vision and pattern recognition*, pages 9924–9935, 2022. 2, 5, 6, 7, 17
- [20] Lukas Hoyer, Dengxin Dai, and Luc Van Gool. Hrda: Context-aware high-resolution domain-adaptive semantic segmentation. In *European conference on computer vision*, pages 372–391. Springer, 2022. 2, 5, 6, 7, 17
- [21] Edward J Hu, yelong shen, Phillip Wallis, Zeyuan Allen-Zhu, Yuanzhi Li, Shean Wang, Lu Wang, and Weizhu Chen. LoRA: Low-rank adaptation of large language models. In *International Conference on Learning Representations*, 2022. 1, 2, 4
- [22] Sadeep Jayasumana, Srikumar Ramalingam, Andreas Veit, Daniel Glasner, Ayan Chakrabarti, and Sanjiv Kumar. Rethinking fid: Towards a better evaluation metric for image generation. In *Proceedings of the IEEE/CVF Conference on Computer Vision and Pattern Recognition*, pages 9307–9315, 2024. 7, 2
- [23] Yuru Jia, Lukas Hoyer, Shengyu Huang, Tianfu Wang, Luc Van Gool, Konrad Schindler, and Anton Obukhov. Dginstyle: Domain-generalizable semantic segmentation with image diffusion models and stylized semantic control. In *Synthetic Data for Computer Vision Workshop@ CVPR 2024*, 2023. 1, 2, 5, 13, 17
- [24] Aliasghar Khani, Saeid Asgari Taghanaki, Aditya Sanghi, Ali Mahdavi Amiri, and Ghassan Hamarneh. Slime: Segment like me. *arXiv preprint arXiv:2309.03179*, 2023. 5
- [25] Dongseob Kim, Seungho Lee, Junsuk Choe, and Hyunjung Shim. Weakly supervised semantic segmentation for driving

- scenes. In *Proceedings of the AAAI Conference on Artificial Intelligence*, pages 2741–2749, 2024. 10
- [26] Diederik P Kingma. Adam: A method for stochastic optimization. *arXiv preprint arXiv:1412.6980*, 2014. 16
- [27] Dawid Jan Kopiczko, Tijmen Blankevoort, and Yuki Markus Asano. Vera: Vector-based random matrix adaptation. *arXiv preprint arXiv:2310.11454*, 2023. 2
- [28] Yoonho Lee, Annie S Chen, Fahim Tajwar, Ananya Kumar, Huaxiu Yao, Percy Liang, and Chelsea Finn. Surgical fine-tuning improves adaptation to distribution shifts. *arXiv preprint arXiv:2210.11466*, 2022. 2
- [29] Daiqing Li, Huan Ling, Seung Wook Kim, Karsten Kreis, Sanja Fidler, and Antonio Torralba. Bigdatasetgan: Synthesizing imagenet with pixel-wise annotations. In *Proceedings of the IEEE/CVF Conference on Computer Vision and Pattern Recognition*, pages 21330–21340, 2022. 1, 2
- [30] Shih-Yang Liu, Chien-Yi Wang, Hongxu Yin, Pavlo Molchanov, Yu-Chiang Frank Wang, Kwang-Ting Cheng, and Min-Hung Chen. Dora: Weight-decomposed low-rank adaptation. *arXiv preprint arXiv:2402.09353*, 2024. 2
- [31] Ilya Loshchilov and Frank Hutter. Decoupled weight decay regularization. In *International Conference on Learning Representations*, 2019. 15, 16, 17
- [32] Sourab Mangrulkar, Sylvain Gugger, Lysandre Debut, Younes Belkada, Sayak Paul, and Benjamin Bossan. Peft: State-of-the-art parameter-efficient fine-tuning methods. <https://github.com/huggingface/peft>, 2022. 13
- [33] Gerhard Neuhold, Tobias Ollmann, Samuel Rota Bulo, and Peter Kontschieder. The mapillary vistas dataset for semantic understanding of street scenes. In *Proceedings of the IEEE international conference on computer vision*, pages 4990–4999, 2017. 5, 6
- [34] Quang Nguyen, Truong Vu, Anh Tran, and Khoi Nguyen. Dataset diffusion: Diffusion-based synthetic data generation for pixel-level semantic segmentation. *Advances in Neural Information Processing Systems*, 36, 2024. 3
- [35] Minh Park, Jooyeol Yun, Seunghwan Choi, and Jaegul Choo. Learning to generate semantic layouts for higher text-image correspondence in text-to-image synthesis. In *Proceedings of the IEEE/CVF International Conference on Computer Vision*, pages 7591–7600, 2023. 1, 2
- [36] Adam Paszke, Sam Gross, Francisco Massa, Adam Lerer, James Bradbury, Gregory Chanan, Trevor Killeen, Zeming Lin, Natalia Gimelshein, Luca Antiga, et al. Pytorch: An imperative style, high-performance deep learning library. *Advances in neural information processing systems*, 32, 2019. 13
- [37] Dustin Podell, Zion English, Kyle Lacey, Andreas Blattmann, Tim Dockhorn, Jonas Müller, Joe Penna, and Robin Rombach. Sdxl: Improving latent diffusion models for high-resolution image synthesis. *arXiv preprint arXiv:2307.01952*, 2023. 1, 2, 5, 6, 11, 13, 15
- [38] Alec Radford, Jong Wook Kim, Chris Hallacy, Aditya Ramesh, Gabriel Goh, Sandhini Agarwal, Girish Sastry, Amanda Askell, Pamela Mishkin, Jack Clark, et al. Learning transferable visual models from natural language supervision. In *International conference on machine learning*, pages 8748–8763. PMLR, 2021. 7
- [39] Aditya Ramesh, Prafulla Dhariwal, Alex Nichol, Casey Chu, and Mark Chen. Hierarchical text-conditional image generation with clip latents. *arXiv preprint arXiv:2204.06125*, 1(2):3, 2022. 2
- [40] Adithya Renduchintala, Tugrul Konuk, and Oleksii Kuchaiev. Tied-LoRA: Enhancing parameter efficiency of LoRA with weight tying. In *Proceedings of the 2024 Conference of the North American Chapter of the Association for Computational Linguistics: Human Language Technologies (Volume 1: Long Papers)*, 2024. 4
- [41] Robin Rombach, Andreas Blattmann, Dominik Lorenz, Patrick Esser, and Björn Ommer. High-resolution image synthesis with latent diffusion models. In *Proceedings of the IEEE/CVF conference on computer vision and pattern recognition*, pages 10684–10695, 2022. 1, 2, 3, 4, 5, 11
- [42] Nataniel Ruiz, Yuanzhen Li, Varun Jampani, Yael Pritch, Michael Rubinstein, and Kfir Aberman. Dreambooth: Fine tuning text-to-image diffusion models for subject-driven generation. In *Proceedings of the IEEE/CVF conference on computer vision and pattern recognition*, pages 22500–22510, 2023. 2
- [43] Chitwan Saharia, William Chan, Saurabh Saxena, Lala Li, Jay Whang, Emily L Denton, Kamyar Ghasemipour, Raphael Gontijo Lopes, Burcu Karagol Ayan, Tim Salimans, et al. Photorealistic text-to-image diffusion models with deep language understanding. *Advances in Neural Information Processing Systems*, 35:36479–36494, 2022. 1, 2
- [44] Christos Sakaridis, Dengxin Dai, and Luc Van Gool. Guided curriculum model adaptation and uncertainty-aware evaluation for semantic nighttime image segmentation. In *Proceedings of the IEEE/CVF international conference on computer vision*, pages 7374–7383, 2019. 5, 6
- [45] Christos Sakaridis, Dengxin Dai, and Luc Van Gool. Acdc: The adverse conditions dataset with correspondences for semantic driving scene understanding. In *Proceedings of the IEEE/CVF International Conference on Computer Vision*, pages 10765–10775, 2021. 2, 5, 6, 7, 8
- [46] Christoph Schuhmann, Romain Beaumont, Richard Vencu, Cade Gordon, Ross Wightman, Mehdi Cherti, Theo Coombes, Aarush Katta, Clayton Mullis, Mitchell Wortsman, et al. Laion-5b: An open large-scale dataset for training next generation image-text models. *Advances in Neural Information Processing Systems*, 35:25278–25294, 2022. 1, 2
- [47] Joonghyuk Shin, Minguk Kang, and Jaesik Park. Fill-up: Balancing long-tailed data with generative models. *arXiv preprint arXiv:2306.07200*, 2023. 1
- [48] Wilhelm Tranheden, Viktor Olsson, Juliano Pinto, and Lennart Svensson. Dacs: Domain adaptation via cross-domain mixed sampling. In *Proceedings of the IEEE/CVF winter conference on applications of computer vision*, pages 1379–1389, 2021. 17
- [49] Patrick von Platen, Suraj Patil, Anton Lozhkov, Pedro Cuenca, Nathan Lambert, Kashif Rasul, Mishig Davaadorj, Dhruv Nair, Sayak Paul, William Berman, Yiyi Xu, Steven Liu, and Thomas Wolf. Diffusers: State-of-the-art diffu-

- sion models. <https://github.com/huggingface/diffusers>, 2022. 13
- [50] Haofan Wang, Qixun Wang, Xu Bai, Zekui Qin, and Anthony Chen. Instantstyle: Free lunch towards style-preserving in text-to-image generation. *arXiv preprint arXiv:2404.02733*, 2024. 2
- [51] Weijia Wu, Yuzhong Zhao, Hao Chen, Yuchao Gu, Rui Zhao, Yefei He, Hong Zhou, Mike Zheng Shou, and Chunhua Shen. Datasetdm: Synthesizing data with perception annotations using diffusion models. *Advances in Neural Information Processing Systems*, 36:54683–54695, 2023. 1, 2, 3, 4, 5, 6, 10, 12, 16
- [52] Weijia Wu, Yuzhong Zhao, Mike Zheng Shou, Hong Zhou, and Chunhua Shen. Diffumask: Synthesizing images with pixel-level annotations for semantic segmentation using diffusion models. In *Proceedings of the IEEE/CVF International Conference on Computer Vision*, pages 1206–1217, 2023. 1, 3, 5
- [53] Yichao Wu, Yafei Xiang, Shuning Huo, Yulu Gong, and Penghao Liang. Lora-sp: Streamlined partial parameter adaptation for resource-efficient fine-tuning of large language models, 2024. 4
- [54] Enze Xie, Wenhai Wang, Zhiding Yu, Anima Anandkumar, Jose M Alvarez, and Ping Luo. Segformer: Simple and efficient design for semantic segmentation with transformers. *Advances in neural information processing systems*, 34: 12077–12090, 2021. 6, 17
- [55] Peng Xing, Haofan Wang, Yanpeng Sun, Qixun Wang, Xu Bai, Hao Ai, Renyuan Huang, and Zechao Li. Csgo: Content-style composition in text-to-image generation. *arXiv preprint arXiv:2408.16766*, 2024. 2
- [56] Lihe Yang, Xiaogang Xu, Bingyi Kang, Yinghuan Shi, and Hengshuang Zhao. Freemask: Synthetic images with dense annotations make stronger segmentation models. *Advances in Neural Information Processing Systems*, 36, 2024. 1
- [57] Fisher Yu, Haofeng Chen, Xin Wang, Wenqi Xian, Yingying Chen, Fangchen Liu, Vashisht Madhavan, and Trevor Darrell. Bdd100k: A diverse driving dataset for heterogeneous multitask learning. In *Proceedings of the IEEE/CVF conference on computer vision and pattern recognition*, pages 2636–2645, 2020. 5, 6
- [58] Qingru Zhang, Minshuo Chen, Alexander Bukharin, Nikos Karampatziakis, Pengcheng He, Yu Cheng, Weizhu Chen, and Tuo Zhao. Adalora: Adaptive budget allocation for parameter-efficient fine-tuning. *arXiv preprint arXiv:2303.10512*, 2023. 4
- [59] Yuxuan Zhang, Huan Ling, Jun Gao, Kangxue Yin, Jean-Francois Lafleche, Adela Barriuso, Antonio Torralba, and Sanja Fidler. Datasetgan: Efficient labeled data factory with minimal human effort. In *Proceedings of the IEEE/CVF Conference on Computer Vision and Pattern Recognition*, pages 10145–10155, 2021. 1, 2, 5
- [60] Hongbo Zhao, Bolin Ni, Junsong Fan, Yuxi Wang, Yuntao Chen, Gaofeng Meng, and Zhaoxiang Zhang. Continual forgetting for pre-trained vision models. In *Proceedings of the IEEE/CVF Conference on Computer Vision and Pattern Recognition (CVPR)*, pages 28631–28642, 2024. 4

Concept-Aware LoRA for Domain-Aligned Segmentation Dataset Generation

Supplementary Material

A. Appendix

In the supplementary material, we provide additional analyses, experiments, qualitative and quantitative results, and implementation details, including pseudocode, due to space limitations in the main manuscript. Specifically, we present an extensive additional analysis of concept sensitivity (Section B) and Concept-Aware LoRA (Section C). We then demonstrate the generalizability of the proposed method using a general-domain dataset, Pascal VOC [12] (Section D). Additionally, we discuss class-aware dataset generation, which could be a promising future research direction for handling long-tailed distributions by leveraging text prompts (Section F). Finally, we provide additional quantitative and qualitative results (Section E) and detailed implementation details, including PyTorch-like pseudocode, to ensure reproducibility. Below is the table of contents for the supplementary material (Section G).

B. Additional Analysis of Concept Sensitivity	1
B.1. The Implicit Bias of Gradients Across Layers	1
B.2. Concept Sensitivity According to the Noise Timestep	1
B.3. Concept Sensitivity According to the Prompt Augmentation	2
C. Additional Analysis of Concept-Aware LoRA	4
D. In-domain Experiments for the General Domain Dataset (Pascal-VOC)	5
D.1. Experimental setup	6
D.2. Quantitative and Qualitative Results	6
E. Additional Qualitative and Quantitative Results	6
E.1. Comparison of Image-Label Alignment	6
E.2. Additional Analysis of Our Generated Dataset on the Domain Generalization Setting	7
E.3. Additional Qualitative Results	9
F. Class-Specific Dataset Generation	10
F.1. Class-wise Segmentation Performance	10
F.2. Generating Datasets with Diverse Class Names	10
G. Implementation Details	10
G.1. Label Generator Architecture	10
G.2. Detailed Architecture of CA-LoRA	12
G.3. Hyperparameters and Pseudocode	13

B. Additional Analysis of Concept Sensitivity

B.1. The Implicit Bias of Gradients Across Layers

Observation (Fig. 6 (a)) We compute the sensitivity scores for each layer by using the norm of the gradient. However, the gradient norm cannot be uniformly scaled across different head types (Q, K, V, OUT), attention types (self, cross), and layers (shallow, deep). To address this, we construct a base gradient to scale the concept loss gradient by referencing the gradient of the original diffusion loss, as described in Section 3.2. We visualize the gradients of both the concept losses and the original diffusion loss in Fig. 6. In this visualization, we separate the self-attention and cross-attention layers to provide clearer distinctions, which differs from the approach in the main paper.

Normalizing Gradients (Fig. 6 (b), Fig. 7) Therefore, we normalize the gradients using the gradients calculated from the original diffusion loss, as discussed in Section 3.2 and shown in Fig. 3. As shown in Fig. 6 (a), the gradients calculated from the style concept loss and viewpoint concept loss are similar. However, the gradient increase ratio can differ significantly, as illustrated in Fig. 6 (b). The final results of the concept sensitivity are visualized in Fig. 7

B.2. Concept Sensitivity According to the Noise Timestep

The amount of added noise, defined by the timestep t , is critical hyperparameter for calculating concept sensitivity. We conduct comprehensive experiments to evaluate concept sensitivity in relation to the noise timestep. Visualizations of concept sensitivity across different noise timesteps, along with qualitative and quantitative results, are provided. These experimental findings offer valuable insights into the behavior of concept sensitivity.

Visualization (Fig. 8) According to our experiment, calculating concept sensitivity at large timesteps (noisy images) does not yield meaningful information about concept sensitivity. For example, style and viewpoint sensitivities appear similar when the timestep is set to 481 out of 1000, as shown in the first column of Fig. 8. This occurs because concept-sensitive layers are less responsive to noisy inputs, which have a high potential to generate any image. Conversely, extremely small timesteps (*e.g.*, 1) also fail to capture concept sensitivity, as the loss from almost clean images does not provide sufficient generative information. Therefore, we explored intermediate timesteps (*e.g.*, 201, 81) and found that the 81st timestep reveals distinct concept sensitivities for style and viewpoint.

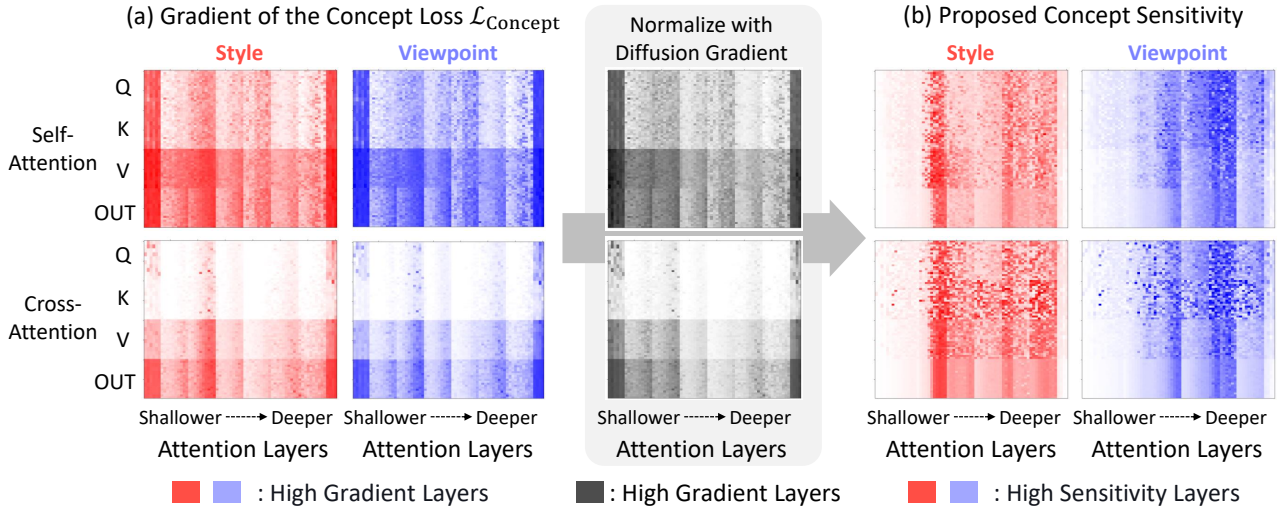


Figure 6. The implicit bias of the gradients across the layers (a). Concept sensitivity is calculated by normalizing each gradient with the gradient of the original diffusion loss (b). We highlight style- and viewpoint-sensitive weights in red and blue, respectively. Each column represents the layer position, ranging from shallow to deep, while each row corresponds to the multi-head projection layers for query, key, value, and output in the attention module.

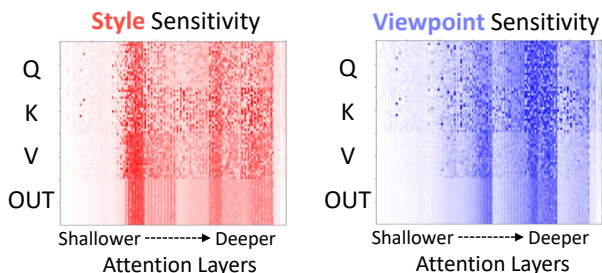


Figure 7. The integrated concept sensitivity of the style- and viewpoint concept sensitivity which we finally used for all experiments.

Qualitative Results (Fig. 9) Additionally, we fine-tuned 2% of the selected ratio using each concept sensitivity and generated images to qualitatively compare results across different noise timesteps. As shown in Fig. 9, the images generated using intermediate timesteps (201, 81) better align with the intended style and viewpoint.

Quantitative Results (Table 5) Finally, we quantitatively compared the intermediate timesteps using the image domain alignment metric, CMMD (\downarrow) [22], to evaluate the 201st and 81st timesteps. The results indicate that the 81st timestep is the most effective for measuring concept sensitivity, as shown in Table 5. While our approach selects a single timestep to measure concept sensitivity, averaging multiple timesteps could improve the precision and robustness of concept sensitivity, which may be a promising direction for future research.

Extracted Timestep	481	201	81	1
Style	1.920	1.556	1.420	2.383
Viewpoint	1.626	2.132	2.313	2.555

Table 5. The CMMD (\downarrow) [22] of the 2% concept-CA-LoRA (style, viewpoint) is evaluated across the extracted timesteps.

B.3. Concept Sensitivity According to the Prompt Augmentation

We conduct an additional analysis of the robustness of defining desired concepts based on prompt augmentation. As demonstrated in Section 3.2, we select several hand-crafted prompt augmentations tailored to the desired concept. While this method is flexible and can be generalized to different concepts, it may introduce vulnerabilities in prompt augmentation. To assess its robustness, we measure sensitivity across various prompt augmentations. Specifically, we provide five prompt augmentations for each desired concept (style, viewpoint) derived from the original prompts, as shown below.

$$c_{\text{Aug(Style)}} \in \left\{ \begin{array}{l} \text{“Sketch of first-person urban street view”}, \\ \text{“Watercolor of first-person urban street view”}, \\ \text{“Pop-art of first-person urban street view”}, \\ \text{“Line art of first-person urban street view”}, \\ \text{“Oil painting of first-person urban street view”} \end{array} \right\} \quad (8)$$

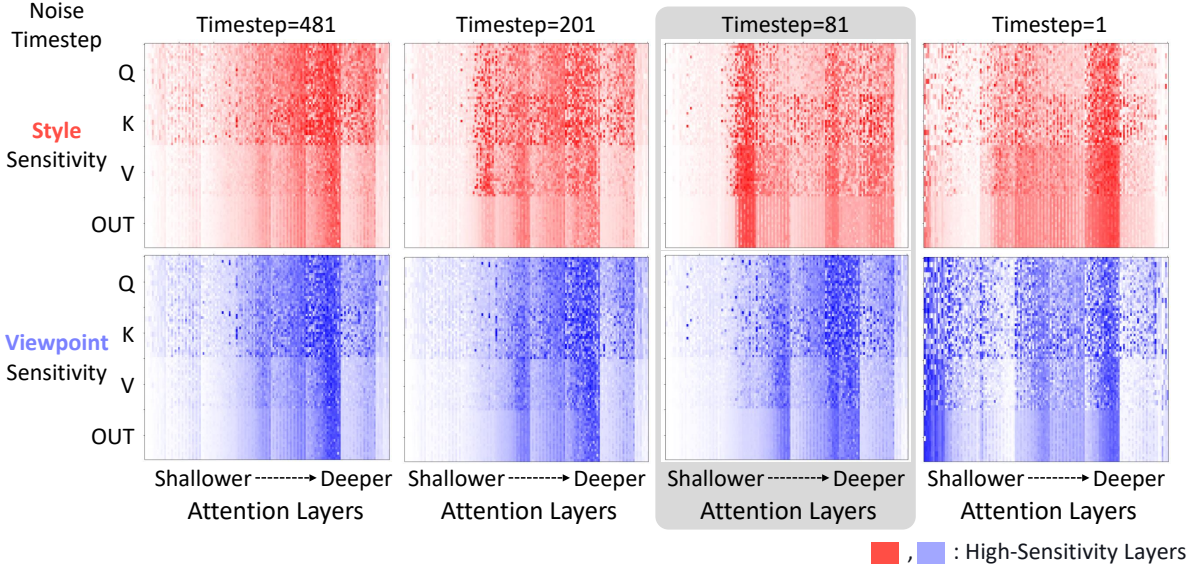


Figure 8. Visualizing concept sensitivity across different noise timesteps (481, 201, 81, and 1) shows that the 81st timestep stands out with a significantly distinct concept sensitivity score between style and viewpoint sensitivity compared to the other timesteps.

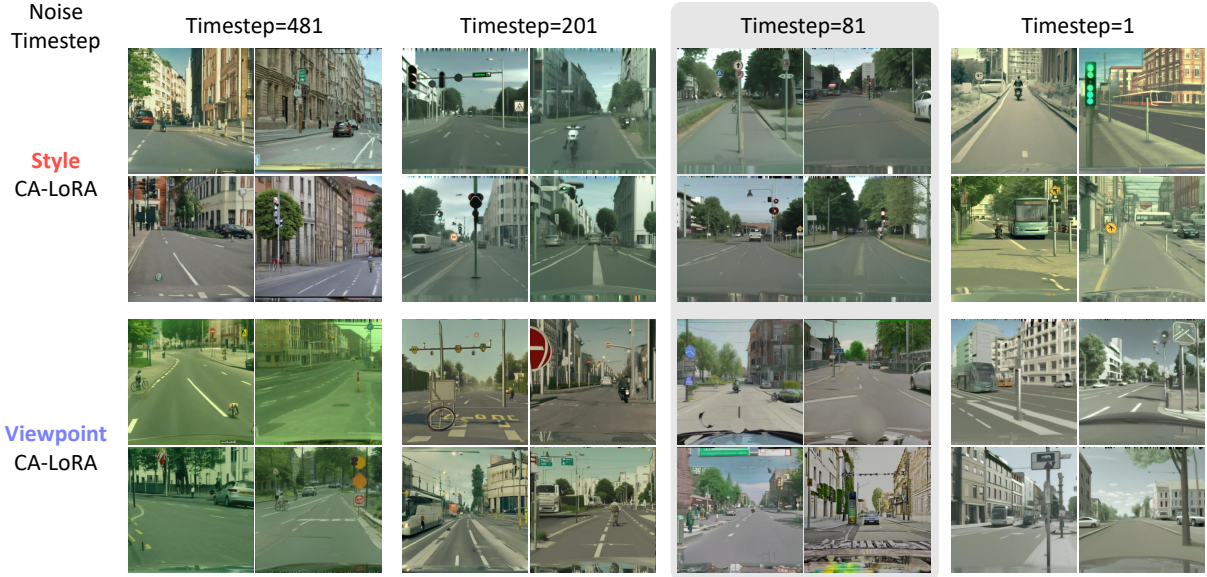


Figure 9. According to the various noise timestep, 81st timestep represents the best concept sensitivity, qualitatively. The style of the generated images by Style CA-LoRA is well-aligned, while the generated images by Viewpoint CA-LoRA contain diverse styles.

$$c_{\text{Aug}(\text{Viewpoint})} \in \left\{ \begin{array}{l} \text{“Photorealistic urban street in top-down view”}, \\ \text{“Photorealistic urban street in high angle view”}, \\ \text{“Photorealistic urban street in low angle view”}, \\ \text{“Photorealistic urban street in eye-level view”}, \\ \text{“Photorealistic urban street in close-up view”} \end{array} \right\} \quad (9)$$

We then calculate the style and viewpoint sensitivity for each prompt augmentation, as shown in Fig. 10. As illustrated in the figure, our proposed method consistently demonstrates high sensitivity to similar regions across all prompt augmentations for styles. Similarly, for viewpoints, augmentations such as top-down, high-angle, and low-angle were applied, and the results indicate that our method highlights similar regions regardless of the specific view-

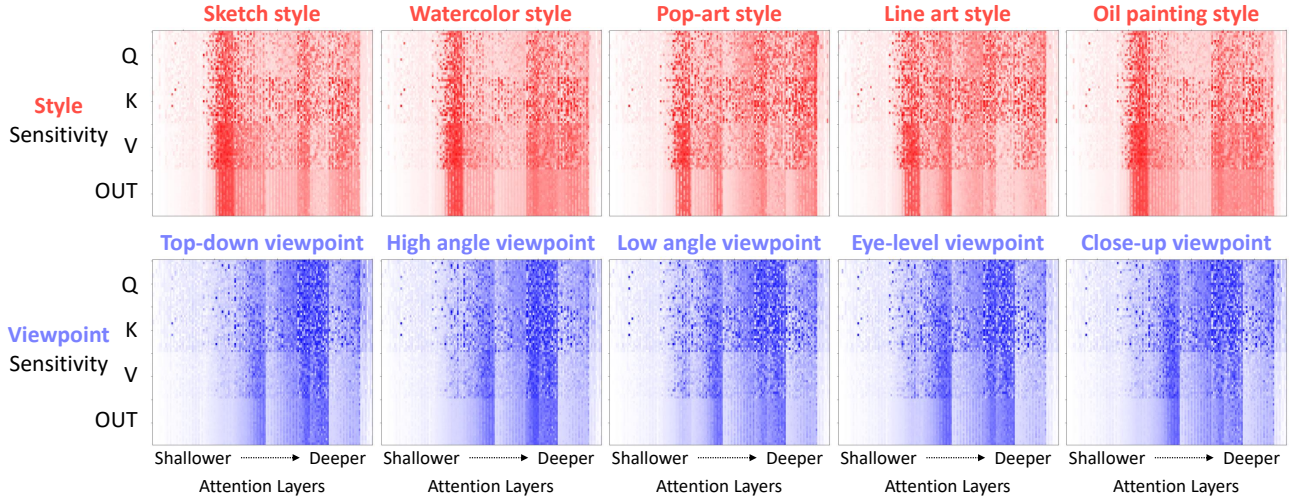


Figure 10. Measured concept sensitivity according to the various prompt augmentation. The highlighted concept-sensitive layers for each concept (style and viewpoint) remained largely consistent regardless of the prompt augmentation, demonstrating the robustness of concept sensitivity to variations in prompt design.

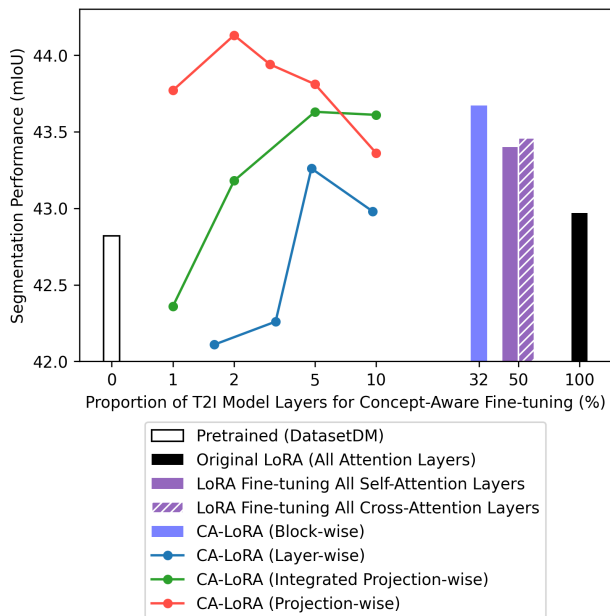


Figure 11. In-domain few-shot semantic segmentation comparison (0.3% Cityscapes) with the hand-crafted layer selection approaches and the variants of CA-LoRA that partition the base weights differently.

point prompt. Based on these findings, we manually select the first three prompts for each desired concept. Nevertheless, developing an automated approach to search for prompt augmentations by leveraging recent LLMs could be a promising direction for enhancing concept sensitivity.

C. Additional Analysis of Concept-Aware LoRA

In this section, we evaluate the effectiveness of our sensitive weight identification method in capturing the desired concepts by comparing its performance against variants of hand-crafted layer selection methods. Additionally, we show the performance of variants of CA-LoRA by changing the granularity of basic component differently (e.g., block, layer). Specifically, we compare our projection-wise CA-LoRA with block-wise, layer-wise, and integrated projection-wise approaches by analyzing their impact on in-domain semantic segmentation performance.

Experimental setup The experimental setup follows the in-domain semantic segmentation experiment presented in Section 4.2. To enhance performance, we generate a segmentation dataset using 0.3% of the labeled Cityscapes dataset [9]. For the hand-crafted manual selection baselines, we include LoRA fine-tuning methods that selectively update all self-attention and cross-attention layers, respectively. Since Stable Diffusion XL contains an equal number of self-attention and cross-attention layers, each hand-crafted selection method fine-tunes 50% of the total layers.

To ensure a comprehensive comparison, we also evaluate “DatasetDM”, which utilizes the pretrained model without fine-tuning, and “Original LoRA”, which applies LoRA fine-tuning to all attention layers. Additionally, we explore the granularity of CA-LoRA while maintaining the same concept awareness across block-wise, layer-wise, integrated projection-wise, and projection-wise approaches. Here, “integrated projection-wise” refers to using a single LoRA matrix for all multi-head attention projections. The detailed



Figure 12. Qualitative comparison with the hand-crafted layer selection approaches by generating a “bus” class. While hand-crafted layer selection approaches, and Original LoRA generate similar bus images with the training bus images, we can generate diverse bus images with well-aligned label maps.

implementation of projection-wise CA-LoRA is provided in Section G.2, which may help differentiate it from integrated projection-wise CA-LoRA.

Comparison with Hand-crafted Layer Selection Approaches (Figs. 11 and 12) As shown in Fig. 11, finetuning only the self- or cross-attention layers outperform DatasetDM and Original LoRA. However, their performance does not reach the level of our Style CA-LoRA, which specifically targets the Style-Sensitive Layers in Cityscapes. To analyze this, we provide examples of bus samples generated using the prompt “photorealistic first-person urban street view *with bus*.” across LoRA finetuning methods for hand-crafted layer selections (self- and cross-attention layers), Original LoRA, and our Style CA-LoRA. As illustrated in Fig. 12, the images of buses seen during training are limited to the top two examples. In the case of hand-crafted layer selection approaches, and Original LoRA, the generated buses closely resemble those seen during training, showing minimal variation. In contrast, our Style CA-LoRA, which selectively fine-tunes only the Style-Sensitive Layers, is capable of generating a diverse range of buses while maintaining the Cityscapes style. We suppose that the diversity in the generated dataset of our method significantly contributed to the superior final performance improvements in semantic segmentation.

Granularity of the Concept-Aware LoRA (Fig. 11) We explore the performance of CA-LoRA variants that partition the base weights differently. As shown in Fig. 11, these variants generally outperform the baselines. Among them, projection-wise CA-LoRA achieves the highest performance compared to other variants. This suggests that increasing the granularity of the base partition generally enhances performance, as it allows for more fine-grained selection of sensitive weights.

D. In-domain Experiments for the General Domain Dataset (Pascal-VOC)

Since our primary goal is to cover urban-scene segmentation, we focused on style and viewpoint as the desired concepts and conducted experiments exclusively on urban-scene datasets such as Cityscapes. However, the CA-LoRA methodology is not limited to urban-scene datasets. It can also be applied to general datasets for in-domain segmentation dataset generation. In this section, we demonstrate experiments on the Pascal-VOC dataset [12], showcasing how our approach improves few-shot semantic segmentation performance.

D.1. Experimental setup

In this experiment, we trained on a total of 100 real image-label pairs and evaluated the model using the 1,449 images in the Pascal-VOC validation set. For the text-to-image generation model, we applied the same style sensitivity score used in the Cityscapes experiment, setting the selected proportion to 10%. During the training of the text-to-image generation model, the prompt "a photo" was used. For training the label generator and generating the dataset, the prompt "a photo of a {class names}" was employed. The label generator was trained with a batch size of 4 for 90K iterations, ultimately producing 2,000 image-label pairs. When utilizing the generated dataset, the process was consistent with the in-domain semantic segmentation experiments. Specifically, Mask2Former was trained on the real dataset for 90K iterations (Baseline), followed by fine-tuning on the combined real and generated dataset for an additional 30K iterations. Additionally, we include an additional fine-tuned baseline (Baseline (FT)) that is solely fine-tuned on the same real dataset for a fair comparison in terms of the total iterations. All other hyper-parameters remained identical to those used in the Cityscapes in-domain semantic segmentation experiment, as detailed in Tables 13 to 15.

D.2. Quantitative and Qualitative Results

As shown in Table 6, using Style CA-LoRA on the Pascal-VOC dataset resulted in a performance improvement of 0.93 mIoU. In contrast, DatasetDM, which omitted the fine-tuning process for the text-to-image generation model, showed a performance drop of 8.43 mIoU. This highlights the importance of concept-aware finetuning for style, even in general datasets beyond urban-scene datasets. Fig. 13 provides further insight into the role of style information. A significant image domain gap is evident between the images generated by the pretrained text-to-image generation model and the dataset generated using Pascal-VOC. This demonstrates the impact of image domain alignment. Quantitatively, the CMMD, which was 1.46 for the pretrained model, decreased to 0.81 after alignment, illustrating the reduced domain gap and its contribution to performance improvement.

E. Additional Qualitative and Quantitative Results

E.1. Comparison of Image-Label Alignment

Quantitative Comparison (Table 7) Since the generated images lack ground-truth label maps, we measure image-label alignment using predictions from a pretrained segmentor. Specifically, we use the predictions from the pretrained Mask2Former model⁴, which was fully supervised on the

⁴<https://github.com/facebookresearch/Mask2Former>

Method	Training Dataset		Total Iterations	Segmentation Performance (mIoU)
	# Real	# Generated		
Baseline	100	X	90K	44.59
For a fair comparison, we fine-tune the baseline for an additional 30K iterations using real or generated datasets.				
Baseline (FT)	100	X	120K	44.39 (-0.20)
DatasetDM	100	2,000	120K	36.16 (-8.43)
Ours	100	2,000	120K	45.52 (+0.93)

Table 6. In-domain segmentation performance (mIoU) of the Pascal-VOC dataset in the few-shot setting (100 image-label pairs). In the first row, we trained Mask2Former on various fractions of the Cityscapes dataset (Baseline). Then, we fine-tuned the baseline on DatasetDM and our generated datasets with 30K iterations and evaluated the performance of the fine-tuned segmentation models. Additionally, we include an additional fine-tuned baseline (Baseline (FT)) that is solely fine-tuned on the same real dataset for a fair comparison in terms of the total iterations.

100% Cityscapes dataset and achieves a 79.40 mIoU, as a proxy for the ground truth mask. Since this method is valid only when the pre-trained segmentor significantly outperforms the label generator, we conduct the image-label alignment experiment in a 0.3% few-shot setting.

Analysis of the Qualitative Comparison (Fig. 5) We compare not only image quality but also image-label alignment across DatasetDM [51], original LoRA, and our Viewpoint- and Style CA-LoRA in the 0.3% few-shot segmentation setting. As shown in the generated labels in Fig. 5, DatasetDM fails to generate corresponding labels, while our Style CA-LoRA generates high-quality corresponding labels. We suppose the reason is grounded by the domain gap between the pretrained T2I model (SDXL [37]) and the source dataset (Cityscapes [9]). As mentioned Section 3.4, DatasetDM trains a label generator using the images of the source domain (*e.g.*, Cityscape images) without performing domain adaptation of the pre-trained T2I model. In other words, the domain gap exists between the label generator and the text-to-image model since the label generator is updated with the Cityscapes images while the original pretrained text-to-image model is not. Due to this domain gap, the intermediate features extracted from the original text-to-image model often fail to reflect the knowledge required for generating label maps of Cityscapes when used as input for the label generator. On the other hand, Style CA-LoRA effectively adapts the T2I model to generate Cityscapes-style images. Therefore, Style CA-LoRA can generate high-quality labels by reducing the domain gap between the intermediate features. However, although the image-label alignment has increased according to the increasing proportions of the selected layers, it does not always provide a better dataset, as shown in our ablation study Table 12 due to the image memorization problem.

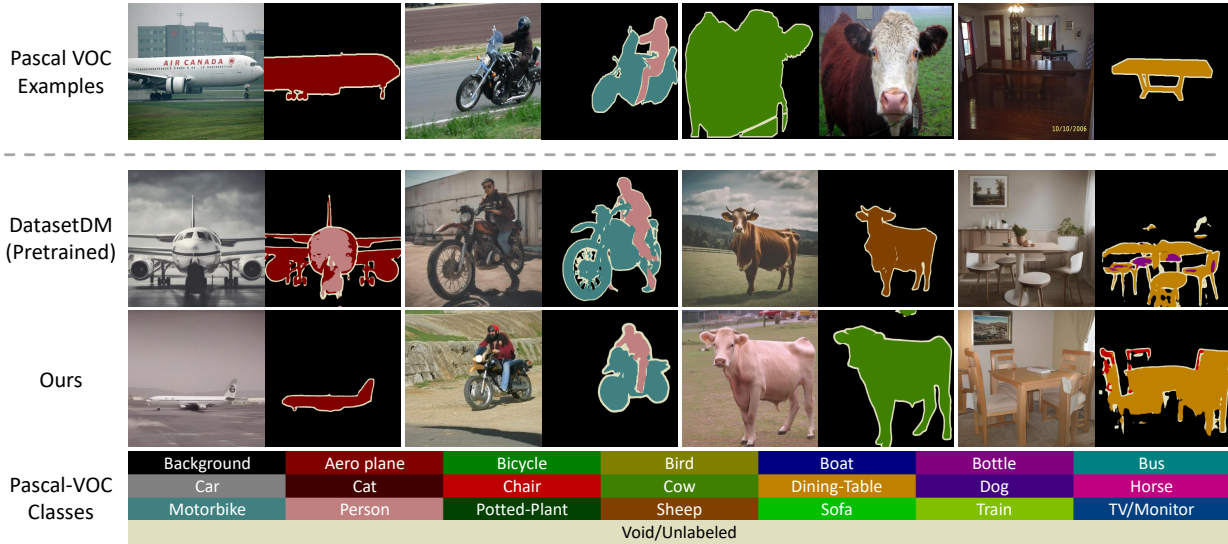


Figure 13. Qualitative comparison for generating Pascal-VOC dataset. Although both DatasetDM and ours are trained on the 100 labeled samples, our generated dataset shows better image domain alignment with the original Pascal-VOC examples and also shows better image-label alignment.

Desired Concept	Proportion of T2I Model Layers for Concept-Aware Fine-tuning						
	0% (Pretrained)	1%	2%	3%	5%	10%	100% (Original LoRA)
Style	25.18	37.01	39.37	40.94	47.84	48.86	60.10
Viewpoint		33.27	29.42	31.44	34.94	38.28	

Table 7. Image-Label Alignment (mIoU) (\uparrow) across the segmentation dataset generation approaches in a few-shot setting (0.3%).

E.2. Additional Analysis of Our Generated Dataset on the Domain Generalization Setting

In this section, we aim to compare and analyze the performance of the Viewpoint CA-LoRA against other baselines that have been applied to urban-scene segmentation in domain generalization. This analysis comprises qualitative assessments (Fig. 14) alongside quantitative evaluations of image domain alignment (Table 8) and image-label alignment (Table 10), similar to Section 4.3 and Section E.1, respectively.

Image Domain Alignment (Table 8 and Fig. 14)

For domain generalization in urban-scene segmentation, we generated urban-scene images under various adverse weather conditions (e.g., “foggy”, “night-time”, “rainy”, and “snowy”). In this section, we assess the domain gap between our generated adverse weather conditions and the real ACDC [45] dataset. Qualitatively, as shown in Fig. 14, our approach generates images that are more realistic and better aligned compared to DatasetDM and InstructPix2Pix, which rely on pretrained models without fine-tuning. When compared to DATUM [4], our method achieves a similar level of image domain alignment while generating more

diverse scenes. Quantitatively, we used CMMD [22] to measure image domain alignment, and the results are presented in Table 8. These results show that the proposed generated dataset demonstrates a significant performance gap over DatasetDM and InstructPix2Pix. More importantly, it achieves competitive performance with DATUM, which requires training *individual models* separately for each weather condition *using a target domain image from the ACDC dataset*.

Image-Label Alignment (Fig. 14 and Tabs. 9 and 10)

We compare image-label alignment to evaluate how reliably label maps are generated for datasets aimed at domain generalization. Qualitatively, as shown in Fig. 14, DATUM generates only images and sets them as pseudo-target domains to apply UDA methods, meaning that no labels are generated. In the case of InstructPix2Pix, style transfer is performed on Cityscapes image-label pairs, using the labels from Cityscapes directly. While this ensures high-quality labels, severe editing can occasionally cause alignment issues, as seen in the foggy examples. Finally, comparing DatasetDM and our method, both of which generate labels directly, shows that our approach achieves significantly better label generation quality compared to DatasetDM.

Method	Foggy	Night-time	Rainy	Snowy	Average
DATUM†	2.41	2.46	2.91	2.10	2.47
InstructPix2Pix	3.43	3.13	2.99	3.32	3.22
DatasetDM	4.90	5.52	5.34	4.96	5.18
Ours	2.43	2.55	2.62	2.63	2.56

Table 8. Comparison of image domain alignment with image generation baselines on four adverse weather conditions. The alignment is measured between the generated images and the ACDC dataset for each weather condition (CMMD ↓). †DATUM trained 4 models for each weather condition in the ACDC dataset, using an additionally provided single target domain image per condition.

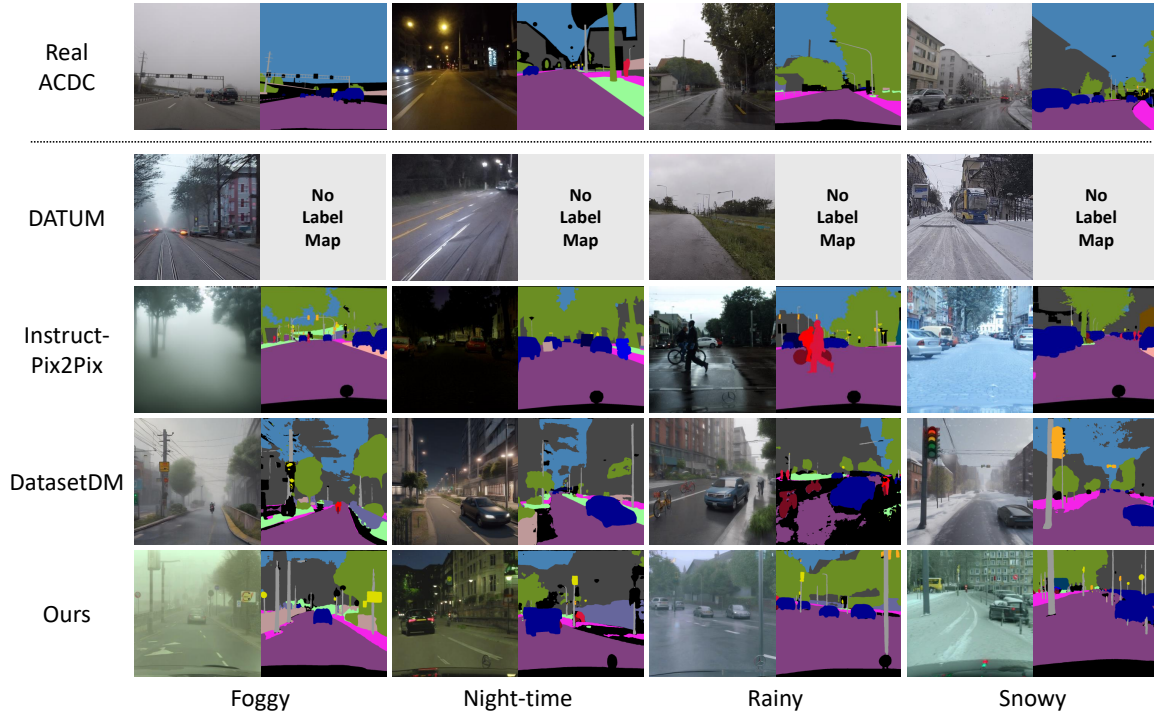


Figure 14. Qualitative results for generating image-label pairs in domain generalization settings. The proposed approach demonstrates its efficacy in both image domain alignment and image-label alignment.

Method	Foggy	Night-time	Rainy	Snowy	Average
Pretrained M2F	67.66	23.17	51.94	47.55	47.58
Finetuned M2F	78.54	52.16	66.23	74.79	67.93

Table 9. Segmentation performance of the Pretrained and Finetuned Mask2Former (M2F) [6] on the adverse weather condition dataset (ACDC [45]). Starting with the pretrained M2F model trained on the Cityscapes dataset [9], we further fine-tuned the model on the ACDC training set for each individual weather condition (learning rate is $3e-6$, the batch size is 2, and the number of iterations is 30K). This approach resulted in highly effective segmentation models tailored to specific weather conditions, serving as pseudo ground-truth masks for evaluating image-label alignment in domain generalization settings.

We then proceed to evaluate image-label alignment quantitatively. As discussed in Section E.1, the generated images lack actual ground truth for domain generalization datasets. Therefore, we rely on pseudo ground truth generated by a highly accurate segmentor. Since no off-the-shelf urban-scene semantic segmentation model consistently performs well across diverse domains, we took several steps

to develop a more reliable segmentor. First, as described in Section E.1, we began with a pretrained Mask2Former (M2F) model trained on the full Cityscapes dataset. However, as shown in Table 9, this model is susceptible to adverse weather conditions. To address this limitation, we fine-tuned the pretrained M2F model individually for each of the four adverse weather conditions in the ACDC train-

Method	Foggy	Night-time	Rainy	Snowy	Average
InstructPix2Pix	25.98	48.60	63.04	40.66	44.57
DatasetDM	40.84	35.90	47.43	44.02	42.05
Ours	41.55	43.07	48.69	39.47	43.20

Table 10. Comparison of image-label alignment with baselines. While InstructPix2Pix provides reliable image-label alignment by fixing Cityscapes labels and applying style transfer only to the weather conditions of the images, its ability to generate diverse scenes is constrained by the fixed labels. In contrast, when comparing methods that generate labels, our approach demonstrates better image-label alignment than DatasetDM.

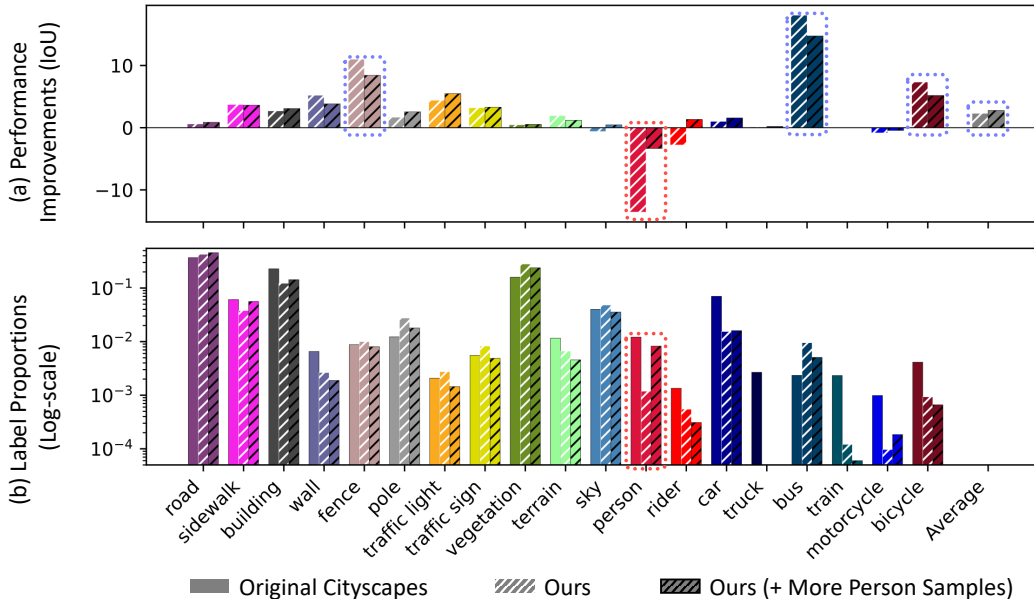


Figure 15. (a) Class-wise performance improvements (IoU) and (b) Label proportions for the original Cityscapes, Ours, and “Ours (+ More Person Samples)”. “Ours (+ More Person Samples)” includes an additional 500 samples for the “person” class to balance the label proportions. As shown in the class-wise performance, significant improvements were achieved for rare classes such as “bus”, “fence”, and “bicycle”, as highlighted by the blue dotted lines. While some classes, such as “person” and “rider”, showed degradation (indicated by red dotted lines), this was due to the lower number of generated samples for these classes. By generating additional samples for these specific classes, a more balanced performance improvement can be achieved, ultimately increasing the overall average performance.

ing set. Since this dataset is not accessible to DatasetDM or our method, the fine-tuned M2F models are guaranteed to outperform those methods. The specific performance improvements on the ACDC validation set are detailed in Table 9.

The results of measuring image-label alignment using the fine-tuned M2F models are presented in Table 10. As shown in the table, InstructPix2Pix, which directly uses Cityscapes labels and only slightly edits the weather conditions of the images, demonstrates an advantage in image-label alignment. Despite its high image-label alignment, we highlighted the limited performance improvements of InstructPix2Pix in Table 2 and Section 4.2, attributing this to the lack of scene diversity caused by its reliance on fixed segmentation label maps. When comparing methods that generate labels, our approach achieves better image-

label alignment than DatasetDM. This improvement stems from our text-to-image generation model learning viewpoints from Cityscapes. As a result, even with the same label generator architecture, our finetuned text-to-image generation model provides representations with a smaller domain gap when generating images based on the Cityscapes dataset.

E.3. Additional Qualitative Results

Additional examples (Figs. 20, 21 and 22) We illustrate the changes in generated images using Style- and Viewpoint CA-LoRA as the proportion of selected layers varies (1%, 2%, 3%, 5%, and 10%). As shown in Fig. 20, both CA-LoRAs effectively focus on the target concept with a small proportion of selected layers. However, as the proportion increases, other concepts are gradually learned, as demon-

strated in the 10% layer selection. For example, the Viewpoint CA-LoRA shows a slight adaptation to the Cityscapes style. This flexibility allows for manual adjustment of the extent to which other concepts are learned, depending on the specific problem settings or datasets.

Furthermore, we provide additional examples of the generated datasets used to improve segmentation performance in fully supervised and domain generalization settings. The additional examples of our generated datasets are available in Figs. 21 and 22.

F. Class-Specific Dataset Generation

F.1. Class-wise Segmentation Performance

In this section, we present a detailed analysis of class-wise improvements, highlighting the effectiveness of the proposed method, particularly for rare classes. Additionally, we introduce a class-balanced performance improvement strategy tailored to specific classes.

Class-wise Performance Improvements (Fig. 15) Urban-scene segmentation has distinct challenges, including class imbalance and co-occurrence issues [25], making class-wise analysis particularly important. We present the class-wise IoU improvements in Fig. 15. As shown in Fig. 15 (a), our proposed dataset generation approach proves especially effective for rare classes such as “bus”, “fence”, and “bicycle”. However, the generated dataset often fails to improve performance in certain classes, such as “person” and “rider”. As illustrated in Fig. 15 (b), this degradation is primarily due to the insufficient number of generated samples for the “person” class. Since the synthetic dataset is generated randomly, disparities in label proportions can occur. To mitigate this, we propose a simple yet effective technique to increase the proportion of the target class.

Segmentation Dataset Generation Focused on a Specific Class (Figs. 15 and 16) As detailed in Section 3.4 and Table 13, we generated the dataset using the prompt “photorealistic first-person urban street view with [Class names]”, where the class names were extracted from the label map of the training set by retrieving the names of all classes present in the label map. While the synthesized text prompt partially reflects the label proportions of the training set, it does not strictly enforce these proportions. As a result, the proposed generated dataset may exhibit misaligned label proportions, as illustrated in Fig. 15 (b).

To address this issue, we propose a class-specific generation approach that manually increases the target class by modifying the generation prompts. Specifically, we generated an additional 500 samples using the prompt “photorealistic first-person urban street view with people” to increase the proportion of the “person” class.⁵ Since we selectively

⁵We also experimented with “photorealistic first-person urban street view with person”, but using “people” as the test prompt proved to be more

fine-tuned the LoRA to learn only the style from Cityscapes, it enables effective manipulation using the text prompt, which the original LoRA cannot achieve, as demonstrated in Fig. 16. As illustrated in Fig. 15 (b), this approach successfully increased the proportion of the “person” class and mitigated its performance degradation. Furthermore, as shown in Fig. 15 (a), this adjustment led to additional performance improvements, increasing the average IoU from 44.12 to 44.59.

F.2. Generating Datasets with Diverse Class Names

Since the Style CA-LoRA selectively fine-tuned only the style from the in-domain Cityscapes dataset, it retains its generalization ability for text prompts such as objects. Leveraging this capability, we aim to generate a broader variety of images using more diverse class names beyond those provided in the dataset. In this experiment, we refined the prompts for generating images previously created with the simple class name “car” by subdividing them into “sedan car”, “SUV car”, “convertible car”, and “hatchback car”, as shown in Fig. 17. As illustrated in the figure, while the original LoRA fine-tuned text-to-image generation model struggles to produce diverse styles of cars, our approach reliably generates a wide variety of cars that align with the test prompts.

We then conducted an in-domain few-shot experiment (Cityscapes 0.3%) using the additional diverse cars dataset, following the experimental setup described in Section 4.1. As shown in Table 11, incorporating the diverse cars dataset significantly improves segmentation performance, particularly for vehicle classes. Beyond generating diverse cars, applying textual augmentations to other class names for dataset creation represents a promising direction for advancing segmentation dataset generation.

G. Implementation Details

G.1. Label Generator Architecture

We build the label generator based on the recent segmentation dataset generation framework, DatasetDM [51]. The label generator in DatasetDM, called P-Decoder, is derived from the Mask2Former [6] decoder architecture. It takes intermediate features from the T2I model, including feature maps and cross-attention maps. The label generator then concatenates features of the same resolution and reduces the feature dimensions using predefined projection layers. The multi-resolution feature maps are passed through the pixel decoder and the transformer decoder sequentially, which outputs the segmentation predictions. Finally, we calculate the loss function of the label decoder, which mirrors that of Mask2Former, incorporating binary cross-entropy, dice loss, and classification loss. However, several modifications

effective in increasing the label proportion for the “person” class.

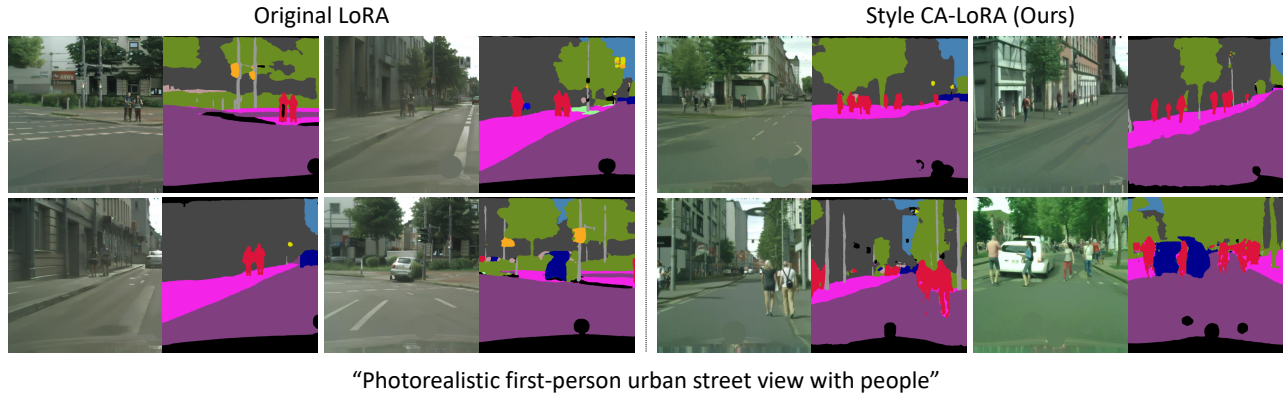


Figure 16. Qualitative comparison between the original LoRA and our Style CA-LoRA for generating the “person” class to increase the label proportion. While the original LoRA can generate the “person” class, it is limited in producing informative samples beyond the training set, with generated images often resembling those from the training set. In contrast, the Style CA-LoRA generates diverse scenes for the “person” class, as it exclusively learns the style from the source dataset.

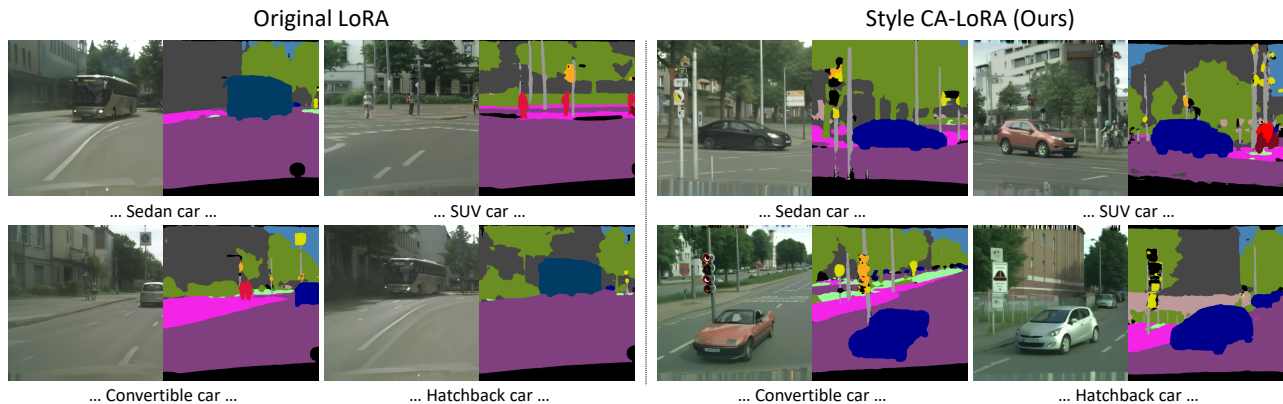


Figure 17. Generated image-label pairs showcasing various styles of cars, including sedan, SUV, convertible, and hatchback. Unlike the Original LoRA, since the Style CA-LoRA exclusively learned only the style from the Cityscapes, we can generate various types of cars in Cityscapes-style.

Method	Training Dataset		Total Iterations	IoU			mIoU
	# Real	# Generated		Car	Bus	Motorcycle	
Baseline	9	✗	90K	84.02	12.51	16.11	41.83
For a fair comparison, we fine-tune the baseline for 30K iterations using the following datasets.							
Baseline (FT)	9	✗	120K	83.98	13.37	15.96	42.00
Ours	9	500	120K	85.03	30.59	15.26	44.12
Ours (+ Diverse Cars)	9	900	120K	85.34	32.48	17.77	44.95

Table 11. In-domain segmentation performance of datasets incorporating the diverse cars dataset. Incorporating the diverse cars dataset especially improved performance for vehicle classes such as “car”, “bus”, and “motorcycle”, leading to overall performance improvements. Since we generated an additional 400 image-label pairs (100 images per vehicle type), the total number of the generated samples is 900.

exist between the original DatasetDM P-Decoder and our label generator due to architectural differences between Stable Diffusion v1.5 [41] and Stable Diffusion XL [37].

Since DatasetDM is built on top of Stable Diffusion v1.5 [41], we simply adjust the feature dimensions in the projection layers to accommodate Stable Diffusion XL [37].

The detailed label generator architecture is illustrated in Fig. 18. However, if all feature maps and cross-attention maps are used, the total number of channels increases significantly, leading to an unmanageable number of parameters in the projection layers during concatenation and projection. In summary, the feature maps are extracted from

Desired Concept	Proportion of T2I Model Layers for Concept-Aware Fine-tuning						
	0% (Pretrained)	1%	2%	3%	5%	10%	100% (Original LoRA)
Style	42.82	43.77	44.13	43.94	43.81	43.36	42.97
Viewpoint		43.13	43.01	42.37	42.94	42.52	

Table 12. Hyperparameter search for the proportion of selected layers in few-shot segmentation (Cityscapes, 0.3%). Style CA-LoRA achieves the best performance with a 2% selection of layers.

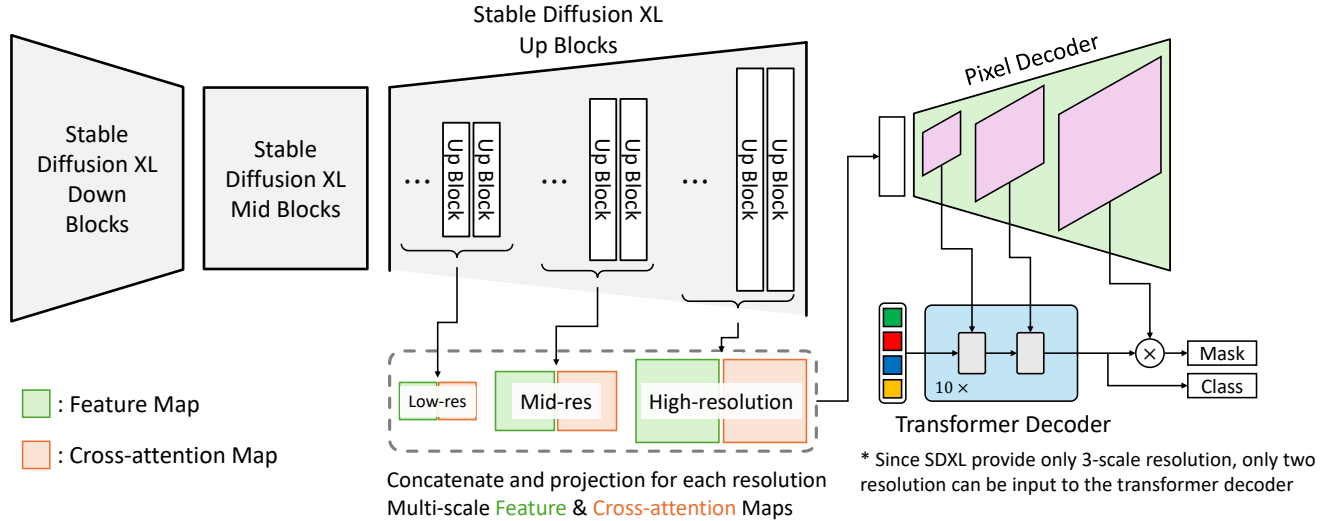


Figure 18. The detailed label generator architecture. The whole framework includes a text-to-image generation model (Stable Diffusion XL), pixel decoder, and transformer decoder, followed by DatasetDM [51]. Due to the change in the architecture of the text-to-image generation model, the following pixel decoder and transformer decoder minorly changed (e.g., the number of input channels and the number of blocks).

the *last feature block* at each resolution of the up-sampling blocks, while cross-attention maps are sampled at equal intervals (every 7 blocks) from the total 36 up-sampling blocks (i.e., 1st, 8th, ... 29th, 36th).

Furthermore, as shown in Fig. 18, Stable Diffusion XL has only three resolution levels, compared to four resolution levels of the Stable Diffusion v1.5 architecture in the original DatasetDM. In the Mask2Former structure, feature maps from the pixel decoder, excluding the largest resolution, are fed into the transformer decoder. While the original design used three-resolution feature maps, only two were utilized in this case. Thus, while DatasetDM provides three-resolution feature maps three times for 9 transformer decoder blocks, we provide two-resolution feature maps five times, leading to a total of 10 transformer decoder blocks. *Importantly, to ensure a fair comparison, the reported scores for DatasetDM were obtained using a re-implemented version based on SDXL with the same modifications.*

G.2. Detailed Architecture of CA-LoRA

Overview (Fig. 19 (a)) The fundamental group of weights used to measure concept sensitivity is the linear projection layer. We selectively adapt the pretrained weights layer by layer within the projection layers. Practically, the projection layers in the multi-head attention block are integrated across heads, we split them to structurally distinguish the weights for each projection. Consequently, we attach LoRA layers projection-wise, as shown in Fig. 19.

Projection-wise CA-LoRA (Fig. 19 (b)) There are two types of CA-LoRA: output LoRA projection layers (Type A: Output (OUT)) and input LoRA projection layers (Type B: Query (Q), Key (K), Value (V)). To split the original LoRA layer ($\Delta W = BA$) in projection-wise, the output projection LoRA layers (ΔW_{OUT}) split the A weights row-wise, while the input projection LoRA layers (ΔW_{IN}) split the B weights column-wise, as illustrated in the following equations.

$$\Delta W_{\text{OUT}} = B \begin{bmatrix} A_1 & A_2 & \cdots & A_h \end{bmatrix}, \quad (10)$$

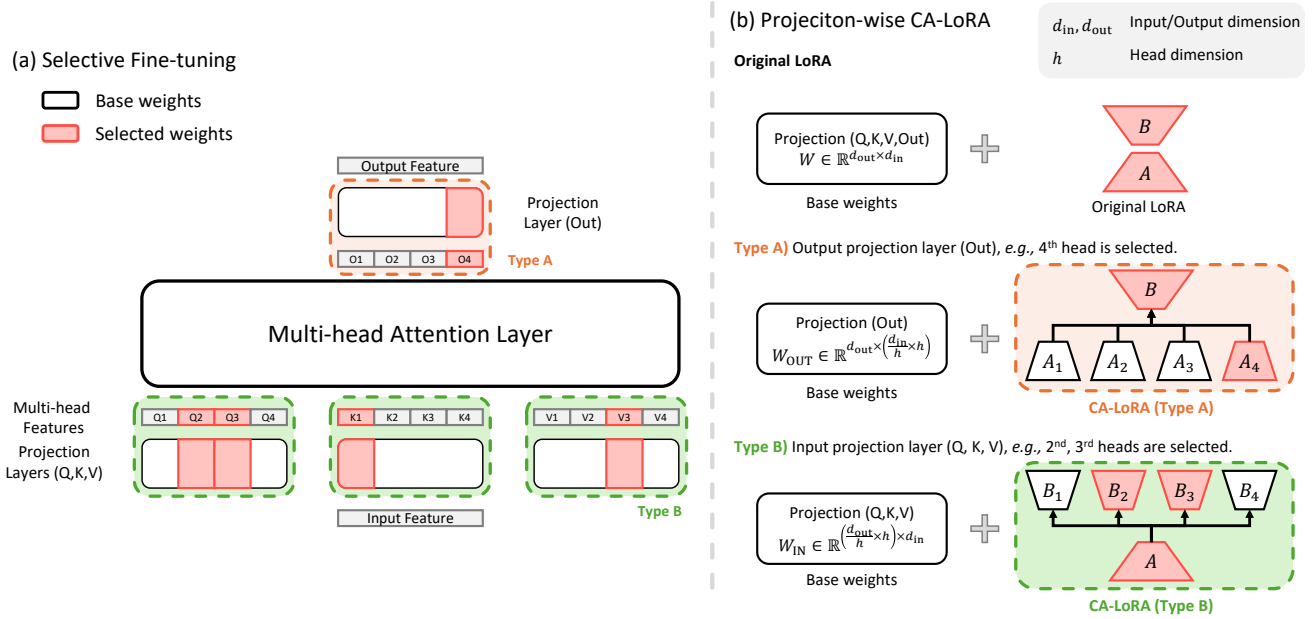


Figure 19. The detailed architecture of the CA-LoRA. We conduct projection-wise CA-LoRA that can attach the LoRA layer for each projection layer of multi-head self-attention.

$$\Delta W_{IN} = \begin{bmatrix} B_1 \\ B_2 \\ \vdots \\ B_h \end{bmatrix} A. \quad (11)$$

The projection-wise LoRA is represented in Fig. 19 and Algorithm 4.

G.3. Hyperparameters and Pseudocode

Hyperparameters (Tables 13, 14, 15 and 16) We provide all hyperparameters to support reproducibility. In the first stage, we fine-tune Stable Diffusion XL [37] using the [HuggingFace Diffusers](#) library [49]. The specific hyperparameters for fine-tuning Stable Diffusion XL on the Cityscapes dataset are listed in Table 13, while the training configurations for the label generator can be found in Table 14.

Next, we train segmentation models for both in-domain and domain generalization scenarios. The hyperparameters for in-domain fine-tuning are provided in Table 15, while those for domain generalization, based on the DGIIn-Style [23] method, are included in Table 16. We hope these provided hyperparameters will facilitate reproducibility.

Pseudocode We also provide PyTorch-like pseudocode [36] for key algorithms to effectively support reproducibility. **Concept sensitivity (Algorithms 1 and 2)** The concept sensitivity algorithm is demonstrated in Algorithm 1. Conducting concept sensitivity requires several helper functions, as shown in Algorithm 2. **CA-LoRA (Algorithms 3 and 4)** The CA-LoRA algorithm is divided into

two parts: the forward function and the declaration function. The forward pass of CA-LoRA is presented in Algorithm 3, while the declaration function, along with the selected layers, is illustrated in Algorithm 4.

While we provide the PyTorch-like pseudocode based on HuggingFace Diffusers library [49], HuggingFace PEFT-based implementation [32] can reduce the training time of the CA-LoRA.



Figure 20. Qualitative results of Style- and Viewpoint CA-LoRA according to the layer proportions (1%, 2%, 3%, 5%, and 10%). While the Style and Viewpoint CA-LoRA effectively disentangle with the small proportions of the selected layers, it has been entangled according to the increased proportion of the selected layers. This flexibility allows for manual adjustment of the extent to which other concepts are learned, depending on the specific problem settings or datasets.

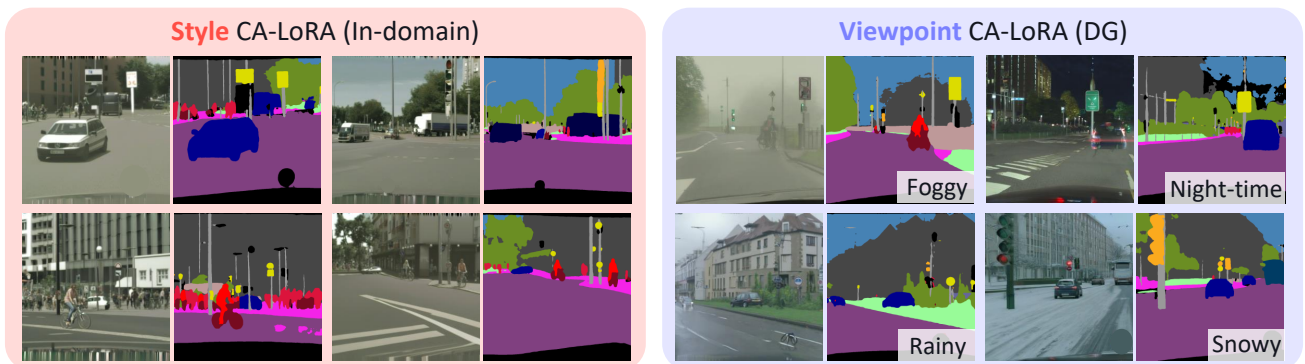


Figure 21. Qualitative examples of the generated image-label pairs for **in-domain** and **domain generalization** settings. Style CA-LoRA effectively generates a Cityscapes-style dataset. Viewpoint CA-LoRA can control the weather condition of the generated images with corresponding label maps since it selectively learns the Cityscapes-viewpoint.

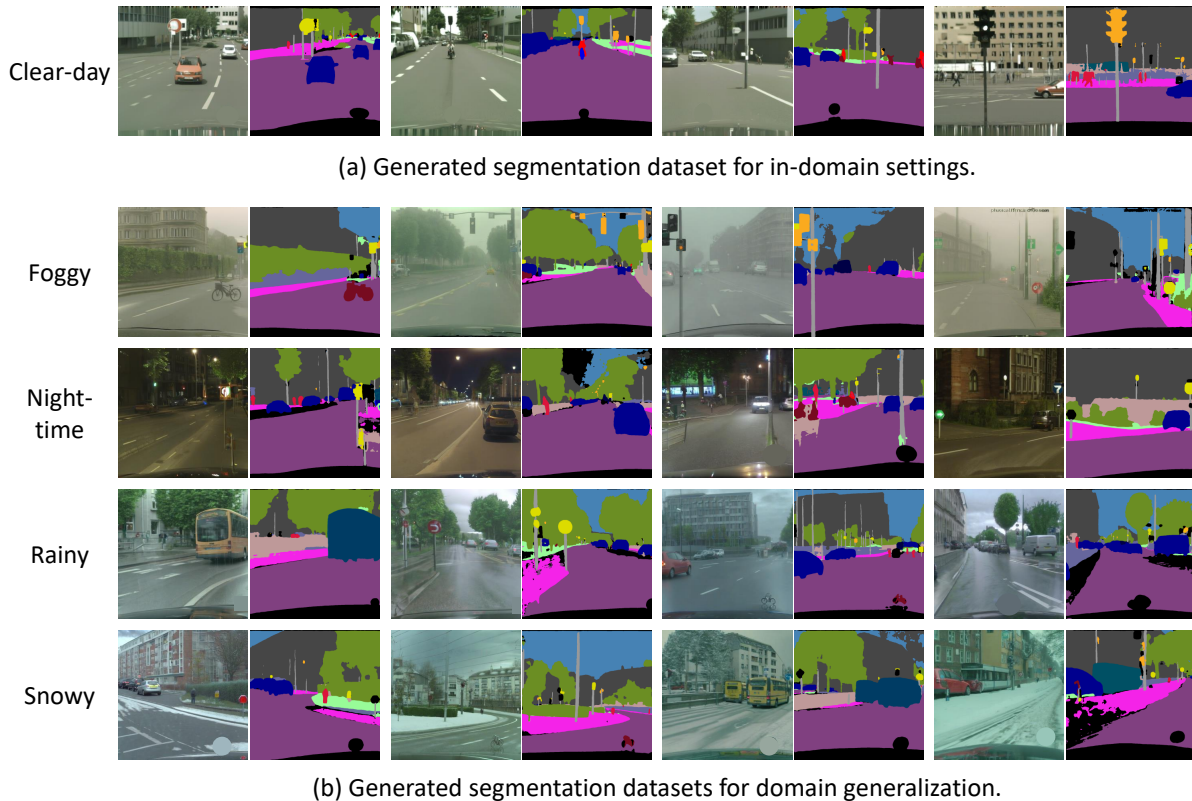


Figure 22. Additional examples of our generated datasets for fully supervised and domain generalization scenarios.

Hyperparameter	Value
Rank	64
Learning rate	1e-4
Batch size	1
Training iteration	10K
Data augmentation	Random horizontal flip, Random crop
Resolution	(1024, 1024)
Learning rate scheduler	constant
Optimizer	AdamW [31]
Adam beta1	0.9
Adam beta2	0.999
Adam weight decay	0.01
Training prompt	“photorealistic first-person urban street view”
Test-time hyperparameters	
Num. inference steps	25
Guidance scale	5.0
Test prompt augmentation (In-domain)	“... with [Class names]” ⁶
Test prompt augmentation (DG)	“... in [Weather Condition] with [Class names]”

Table 13. Hyperparameters to fine-tune Stable Diffusion XL [37]. The class names are extracted from the label map in the training set by retrieving the names of all classes that appear in the label map.

Hyperparameter	Value
Architecture	Mask2Former-shaped label generator [51]
Learning rate	1e-4
Batch size	2 for all few-shot, 8 for fully-supervised
Training iteration (few-shot)	12k, 24k, 24k, and 48k for 0.3%, 1%, 3%, and 10%, respectively
Training iteration (fully-supervised)	90K
Data augmentation	Random horizontal flip, Random resized crop (0.5, 2.0)
Resolution	(1024, 1024)
Learning rate scheduler	PolynomialLR(power=0.9)
Optimizer	Adam [26]
Adam beta1	0.9
Adam beta2	0.999
Adam weight decay	0.0

Table 14. Hyperparameters to train label generator followed by DatasetDM [51].

Hyperparameter	Value
Model Architecture	Mask2Former [6]
Num. generated images	500 for all few-shot, and 3,000 for fully-supervised
Learning rate	3e-6
Batch size	2 for all few-shot, and 8 for fully-supervised
Mixed batch	real:syn = 1:1
Training iteration	30K
Data augmentation	Random horizontal flip, Random resized crop (0.5, 2.0)
Resolution	(512, 1024)
Learning rate scheduler	PolynomialLR(power=0.9)
Optimizer	AdamW [31]
Adam beta1	0.9
Adam beta2	0.999
Adam weight decay	0.05

Table 15. Hyperparameters to fine-tune Mask2Former [6]. We modify the learning rate, batch size and training iteration from the original Mask2Former training configuration.

Hyperparameter	Value (ColorAug) [54]	Value (DAFormer) [19]	Value (HRDA) [20]
Model Architecture	SegFormer	DAFormer	HRDA
Backbone		MiT-B5 [54]	
Num. generated images	500 for each weather condition (clear, foggy, night-time, rainy, and snowy)		
Learning rate		6e-5	
Batch size		2	
Training iteration		40K	
Data augmentation for Gen.	Random horizontal flip, PhotoMetricDistortion		
Data augmentation for Real	Random horizontal flip, Random crop, DACS [48]		
Resolution	(512, 512)	(512, 512)	(1024, 1024)
Learning rate scheduler		PolynomialLR(power=0.9)	
Learning rate warmup		Linear	
Learning rate warmup iteration		1500	
Learning rate warmup ratio		1e-6	
Optimizer		AdamW [31]	
Adam beta1		0.9	
Adam beta2		0.999	
Adam weight decay		0.01	
SHADE	False	True	True
RCS [19, 20]		False	

Table 16. Hyperparameters to train domain generalization in segmentation including ColorAug, DAFormer [19], and HRDA [20], followed by DGINStyle [23].

Algorithm 1 PyTorch-like Pseudocode of Concept Sensitivity

```
# pipe: text-to-image generation diffusers pipeline
# c: str = "photorealistic first-person urban street view"
# c_augs: List[str] = List of the augmented prompts
# t: int = pre-defined timestep
# n_img: int = number of generated images for average

UNET = pipe.unet
UNET = UNET.requires_grad_(True)

# optimizer for clear gradients
optimizer = torch.optim.AdamW(list(filter(lambda p: p.requires_grad, UNET.parameters())))

IMGS = [pipe(c).images[0] for _ in range(n_img)] # generate images

sensitivity = []

for img in IMGS: # average over generated images
    for c_aug in c_augs: # average over augmented captions
        latent = pipe.vae.encode(img)
        noise = torch.randn_like(latent)
        noisy_latent = pipe.scheduler.add_noise(latent, noise, t)

        prompt_embeds = encode_prompt(c)
        model_pred = UNET(noisy_latent, t, prompt_embeds)

        gt_diff = noise

        with torch.no_grad():
            prompt_embeds_aug = encode_prompt(c_aug)
            gt_concept = UNET(noisy_latent, t, prompt_embeds_aug)

        loss_diff = torch.nn.functional.mse_loss(model_pred, gt_diff)
        loss_concept = torch.nn.functional.mse_loss(model_pred, gt_concept)

        loss_diff.backward(retain_graph=True)
        grads_diff = get_UNET_grads(UNET) # Algorithm 2
        optimizer.zero_grad()

        loss_concept.backward()
        grads_concept = get_UNET_grads(UNET) # Algorithm 2
        optimizer.zero_grad()

    sensitivity.append(grads_concept / grads_diff)
sensitivity_avg = average_gradients(sensitivity) # Algorithm 2
```

Algorithm 2 PyTorch-like Helper Functions for Concept Sensitivity

```
def getattr_recursive(module, attrs: List[str]):
    target_module = module
    for attr in attrs:
        target_module = getattr(target_module, attr)
    return target_module

def get_unet_grads(unet):
    grads = {'to.q': [], 'to.k': [], 'to.v': [], 'to.out.0': []}
    for attn_name in unet.attn_processors.keys():
        attn_module = getattr_recursive(unet, attn_name.split('.')[::-1])

        for proj_name in grads.keys():
            proj = getattr_recursive(attn_module, proj_name.split('.'))
            head_dim = 1 if proj_name == 'to.out.0' else 0
            grads_chunk = torch.chunk(proj.weight.grad.cpu(), attn_module.heads, dim=head_dim)
            grads[proj_name].append([(grad ** 2).mean().sqrt().item() for grad in grads_chunk])

    return grads

def average_gradients(grads):
    grad_avg = {'to.q': [], 'to.k': [], 'to.v': [], 'to.out.0': []}

    for key in grad_avg:
        for grad in grads:
            grad_avg[key].append(grad[key])
        grad_avg[key] = torch.mean(torch.tensor(grad_avg[key]), dim=0)

    return grad_avg
```

Algorithm 3 PyTorch-like Pseudocode of Modifying forward function of CA-LoRA

```
# F: torch.nn.functional

def modify_to_ca_lora(layer, reduced_layer):
    # layer: diffusers.models.LoRACompatibleLinear
    # reduced_layer: 'A' or 'B'

    def ca_lora_set_lora_layer(self: LoRACompatibleLinear):
        def set_lora_layer(lora_layer, indices):
            self.lora_layer = lora_layer
            if indices is not None:
                self.indices = indices
            return set_lora_layer

    def ca_lora_set_forward(self: LoRACompatibleLinear):
        def forward(hidden_states: torch.Tensor, scale: float = 1.0):
            if self.lora_layer is None:
                return F.linear(hidden_states, self.weight, self.bias)
            else:
                if self.indices is not None:
                    # CA-LoRA (start)
                    org = F.linear(hidden_states, self.weight, self.bias)
                    if reduced_layer == 'B':
                        org[:, :, self.indices] += scale * self.lora_layer(hidden_states)
                    else:
                        org += scale * self.lora_layer(hidden_states[:, :, self.indices])
                    return org
                # CA-LoRA (end)
            else:
                return F.linear(hidden_states, self.weight, self.bias) + scale *
                    self.lora_layer(hidden_states)
            return forward

    layer.set_lora_layer = ca_lora_set_lora_layer(layer)
    layer.forward = ca_lora_set_forward(layer)

    return layer
```

Algorithm 4 PyTorch-like Pseudocode of selecting projection layers for CA-LoRA

```
def apply_ca_lora(unet, selected_layers, rank):
    for attn_processor_name in unet.attn_processors.keys():
        _selected_layers = [selected_layer for selected_layer in selected_layers if
            '.'.join(attn_processor_name.split('.')[:-1]) in selected_layer]
        if len(_selected_layers) == 0:
            continue
        attn_module = getattr_recursively(unet, attn_processor_name.split('.')[:-1])
        # getattr_recursively: Algorithm 2
        dim_head = attn_module.out_dim // attn_module.heads
        for layer_type in ('to.q', 'to.k', 'to.v', 'to.out.0'):
            selected_layers_proj = [selected_layer for selected_layer in _selected_layers if layer_type in
                selected_layer]
            is_out = layer_type == 'to.out.0'
            if len(selected_layers_proj) == 0:
                continue
            projection_layer = getattr_recursively(attn_module, layer_type.split('.'))
            # getattr_recursively: Algorithm 2

            # Projection-wise CA-LoRA (start)
            head_indices = sorted([int(selected_layer.split('.')[-1][1:]) for selected_layer in
                selected_layers_proj])
            indices = sum([list(range(dim_head * head_idx, dim_head * (head_idx + 1))) for head_idx in
                head_indices], [])
            # Indices are split grouped by the dim_head
            # Projection-wise CA-LoRA (end)

            projection_layer = modify_to_ca_lora_linear(projection_layer, reduced_layer='A' if is_out else
                'B')
            # modify_to_ca_lora_linear: Algorithm 3

            if is_out:
                projection_layer.set_lora_layer(
                    LoRALinearLayer(
                        in_features=len(indices),
                        out_features=projection_layer.out_features,
                        rank=rank),
                    indices)
            else:
                projection_layer.set_lora_layer(
                    LoRALinearLayer(
                        in_features=projection_layer.in_features,
                        out_features=len(indices),
                        rank=rank),
                    indices)

    return unet
```
